

LEGEND







-  Au Anomaly ($\geq 31\text{ppb}$)
-  Cu Anomaly ($\geq 62\text{ppm}$)
-  Pb Anomaly ($\geq 90\text{ppm}$)
-  As Anomaly ($\geq 115\text{ppm}$)
-  Gold-bearing Quartz Vein
-  Drill Hole

Fig. 2-2-4 Distribution of Rock-Chip Geochemical Anomalies in the Da Mai Area

2-4 Geophysical Survey (CSAMT Method)

2-4-1 Outline of Survey

Geophysical survey using CSAMT method was carried out in the Da Mai, Gang and Ngan Me areas in the first phase. The objectives of the survey were to investigate the relationship between resistivity and geologic structure and to extract resistivity anomalies related to mineralization. The Array CSAMT method was employed in this survey.

Amounts of the survey were as follows.

- Total length of survey lines: 30 km
- Survey points: 330 points
- Laboratory test samples: 20 pcs

2-4-2 Survey Method

(1) Methodology

The MT method (Magnetotelluric method) is the exploration to estimate subsurface structure from determining resistivity distribution in the earth. The method uses alternating electromagnetic wave as a signal. Since the depth of sounding is dependent on frequency, the method is capable of exploring from surface to several km in depth by varying the frequency.

The CSAMT (Controlled Source Audio-Frequency Magnetotelluric) method applied to this survey belongs to one of the MT method and measures data in the audio frequency range with artificially controlled source. Recently, the method has been frequently utilized in exploring mineral deposit, geothermal energy, hot spring and groundwater on account of the following advantages.

- S/N ratio can be made higher due to the use of artificially controlled source.
- The measurement can be made more quickly due to the use of high frequencies.
- It is easy to transport the equipment even in steep mountain areas because they are compact and light.

The theory and measurement of the CSAMT method are the same as MT method, with the exception of using artificially controlled source. The Array CSAMT method can carry out the measurement of serial points on a survey line simultaneously.

A set of current electrodes (transmitting dipole) laid out apart from measuring points generates electromagnetic wave as a signal source. The electric field E_x parallel to the transmitting dipole and

the horizontal magnetic field H_y perpendicular to the transmitting dipole are measured at a receiving point. The Array CSAMT method measures the electric field of several points with serial potential electrodes simultaneously. The apparent resistivity of the earth is calculated with these quantities. The equation for this calculation is as follows.

$$\rho_a = (1/5f) \cdot |E_x/H_y|^2 \quad (1)$$

ρ_a : Apparent resistivity (ohm-m)

f : Frequency (Hz)

E_x : Electric field intensity (mV/km)

H_y : Magnetic field intensity (gamma)

To the effective depth of exploration, the skin depth (2) is utilized. It shows the depth where the amplitude of incident electromagnetic wave decays to $1/e$ (37%).

$$\delta = 503 (\rho/f)^{1/2} \quad (2)$$

If a transmitting dipole is near measuring points, the assumption that primary field is plane electromagnetic wave is not held in low frequency range. In this frequency range, MT theory is not able to apply to CSAMT data. This phenomenon is called the Near-Field effect. If the Near-Field effect occurs, apparent resistivity increases monotonously as frequency decreases.

(2) Field Survey

Two sets of transmitting dipole were laid out as shown in a figure in the first phase report. The transmitting dipole No. 1 located approximately 6 km west of the Da Mai area was applied to the measurement of this area. The current electrode No. 2 located approximately 5 km west of the Gang area was applied to the measurement of the Gang and Ngan Me areas. Both dipoles are N-E in direction and about 1.6 km in spacing.

The survey lines (1 km in length, N-E in direction and 200 m in interval) were laid out as shown in figures in the first phase report.

The spacing of measuring points and potential electrodes are 100 m. Ten frequencies of 4, 8, 16, 32, 64, 128, 256, 512, 1,024, and 2,048 Hz were measured. Maximum 6 points were simultaneously measured.

The equipment used in this survey is shown in a table in the first phase report.

(3) Laboratory Test

Resistivity and chargeability of rock samples in the survey areas were measured in laboratory. The same method as in the field measurement was applied. More than twenty samples were measured in laboratory.

(4) Analytical Method

The analysis was carried out according to the flow chart as shown in a figure in the first phase report.

Pseudosection of Apparent Resistivity: In this section, apparent resistivity was plotted for each line. The vertical axis of the section is frequency. The data of higher frequencies were plotted in the upper of the section, and those of lower frequencies were plotted in the lower of the section dependent on the skin depth.

Contour Map of Apparent Resistivity: In this map, the apparent resistivity of the specific frequency was plotted and their contours were drawn.

1-D Inverse Analysis: This analysis assumes that resistivity structure is horizontal multi-layered structure, and determines the optimum parameter (resistivity and thickness) of horizontal multi-layered structure model for each measuring point. The apparent resistivity curve calculated for the optimum model was best fitted to the observed apparent resistivity curve. These parameters were calculated with the non-linear least squares method.

Resistivity Structure Section (1-D Inverse Analysis): In this section, the resistivity column of every measuring point was delineated on each line using the results of the 1-D inverse analysis.

2-D Inverse Analysis: This analysis assumes that resistivity structure is two-dimensional structure, and determines the optimum resistivity distribution of two dimensional model for each line. The distribution of apparent resistivity calculated for the optimum model was best matched to the distribution of the observed apparent resistivity. It was assumed that the CSAMT data in this survey were TM mode data. The finite element method was applied to the forward analysis, and the non-linear least squares method with smoothness constraint was applied to the optimization of resistivity distribution

Resistivity Structure Section (2-D Inverse Analysis): In this section, the resistivity distribution below each line was drawn using the results of the 2-D inverse analysis.

Resistivity Structure Map (2-D Inverse Analysis): In this map, the resistivity distribution at the specific level was drawn using the results of the 2-D inverse analysis.

Integrated Interpretation Map: In this map, the geophysical results were integrated with the geologic information.

2-4-3 Results of Field Survey

(1) Apparent Resistivity

The pseudosections of the apparent resistivity of every line are shown in figures in the first phase report, and the contour maps of the apparent resistivity of 3 frequencies (1,024, 128 and 16 Hz) are shown in figures in the first phase report. The Near-Field effect increasing apparent resistivity monotonously occurred in those of 64 Hz and less. Thus these data were not regarded as the MT information. The apparent resistivity more than 64 Hz on all lines is extremely high (more than 2,000 ohm-m) and little changeful in the pseudosections.

The apparent resistivity of 1,024 and 128 Hz show the similar distribution. The apparent resistivity shows a tendency to be low in the ridge parts and high in the valley parts. The direction of the resistivity distribution, on the whole, is E-W according to the topography. The high resistivity zones more than 5,000 ohm-m were detected in the southern part continuing in the E-W direction, at No. 2 on lines D-1 to D-3, and No. 3 and No. 4 on lines D-7 to D-10.

(2) Resistivity Structure (1-D Analysis)

The 1-D analysis for the Da Mai area was carried out on the data more than 64 Hz which were not Near-Field. The resistivity structure sections drawn with the 1-D analysis are shown in figures in the first phase report. The analysis gave the two-layered structure composed of low resistivity layer in the shallow zone up to the depth of 100~200 m and high resistivity one in the deep zone, as a whole.

(3) Resistivity Structure (2-D Analysis)

The resistivity structure sections drawn with the 2-D analysis are shown in figures in the first phase report. The resistivity structure maps of 3 levels (SL 100m, SL 0m, and SL -200m) are shown in figures in the first phase report. Removing the topographic effect (low resistivity in the ridge parts and high resistivity in the valley part were reduced) made the resistivity distribution more smooth than the apparent resistivity distribution. The analysis gave resistivity more than 2,000 ohm-m to the resistivity

structure, except for the surface in the north-eastern part. On the whole, the relatively low resistivity areas were distributed in the shallow zone up to the depth of 200-300 m and the high resistivity areas were distributed broadly in the deep zone. The high resistivity zones tended to extend to the surface at Nos. 7 and 8 on lines D-3 to D-5, and in the southern part of lines D-7 to D-9.

2-4-4 Laboratory Test

The results of the laboratory test are shown in a table in the first phase report. The mean values of resistivity and chargeability for each rock are as follows.

Rock	Resistivity (ohm-m)	Chargeability (mV/V)
Quartz vein	16,919	25.9
Claystone Siltstone	646	3.9
Shale	1,389	9.8
Sandstone	2,602	13.6
Phyllite	1,726	12.1
Schists	1,716	12.1
Granite	1,734	13.5

The laboratory test offered the result matched to the CSAMT data that the resistivity of the rock samples was higher than 1,000 ohm-m except claystone and siltstone. Especially, the resistivity of the quartz vein was a figure higher (more than 10,000 ohm-m) than that of the other rocks. However, the resistivity of the quartz vein varied widely, depending on the condition of fissures. The samples containing few fissures measured higher than 10,000 ohm-m, while the samples containing remarkable fissures measured a figure lower (about 2,000 ohm-m). The sandstone and schists of the host rock had high resistivity of about 2,000 ohm-m. The granite had the same value as the host rock. However, the samples of the granite were weathered and cataclastic. Thus, the resistivity of the fresh rock in the deep zone would be still higher. Claystone and siltstone were the lowest (about 600 ohm-m) of the rocks in the survey areas. A low resistivity of 600 ohm-m existed in the shale also.

The chargeability of the samples measured about 10 mV/V except quartz vein. The mean value of the quartz vein was 25.9 mV/V. However, the chargeability of the quartz vein varied widely, depending on the existence of pyrite. The samples containing no pyrite measured several mV/V, while the samples containing pyrite measured the largest of 96 mV/V. Relatively large chargeability of about 20 mV/V existed in phyllite and schists. The graphite schist measured small (5.6 mV/V) in chargeability. This small chargeability was due to the sample containing few amounts of graphite. The laboratory test gave the obvious contrast between the quartz vein containing pyrite and the other rocks in the survey areas.

2-4-5 Integrated Interpretation

(1) Resistivity Features

The laboratory test results and geologic information led to the following resistivity features about the rocks and geologic structure in the survey areas.

1) High Resistivity

In the survey areas, the group of quartz veins and the granite are assumed to form higher resistivity than the host rock.

The quartz vein containing few fissures is extremely high (more than 10,000 ohm-m) in resistivity. However, it is very difficult to extract narrow high resistivity zone in width by this measurement system. In the case of the zone where many quartz veins are concentrated (the group of quartz veins), it is sufficiently possible to extract a high resistivity zone related to quartz veins. MT method is not much sensitive to high resistivity. Thus, the width of the group of quartz veins is expected to be more than 100 m if a high resistivity zone related to quartz veins is extracted by this measurement system. When fractures develop in the group of quartz veins, it is possible that the resistivity of the group is lowered and a high resistivity zone related to quartz veins is not extracted.

When the samples of granite were weathered and cataclastic, they had the same resistivity (1,734 ohm-m) as the host rock. When the granite is fresh in deep zone, it seems that granite is several times higher in resistivity and a high resistivity area related to granite is extracted.

The laboratory test shows that the existence of the other rocks might not form higher resistivity.

2) Low Resistivity

In the survey areas, claystone and siltstone, fracture zone and the layer containing graphite are assumed to form lower resistivity than the host rock.

The laboratory test showed that claystone, siltstone and one of the shale had the lowest resistivity (about 600 ohm-m). When fractures exist in these rocks, they lower further their resistivity.

In fracture zones, low resistivity zones are generally extracted, because they are high permeable (high conductible). Many of fracture zones have a figure lower resistivity less than host rock.

Graphite has extremely low resistivity less than several ohm-m. The resistivity of the layer containing graphite is lowered depending on its content.

(2) Relations to Geologic Structure

The figure arranged the resistivity structure sections (2-D analysis) in the sequence of the lines is shown in a figure in the first phase report to grasp three dimensional resistivity structure. The followings are the geological interpretation to resistivity structure in the Da Mai area on the basis of the above resistivity features.

Resistivity structure : The high resistivity areas are distributed broadly below about 300 m from the surface. The high resistivity zones towards the surface were detected and at the Nos. 7 and 8 on lines D-3 to D-5, and in the southern part of lines D-7 to D-9.

Interpretation: The high resistivity areas in the deep zone seem to be reflected by the distribution of granite. The high resistivity zones seem to result from the group of quartz veins or the stock of granite. They are expected to be relatively steep and extend to the deep zone.

(3) IP Method

The laboratory test results gave the obvious contrast between the quartz vein containing pyrite and the other rocks in the survey areas. When the IP method is applied to this areas, it is graphite that adversely affects the data. The laboratory test showed that the IP effect is small, in the case of containing few amounts of graphite. If a layer contains a considerable amount of graphite, the CSAMT method sensitive to low resistivity should extract a low resistivity area because of the extremely low resistivity (less than several ohm-m) of graphite.

Consequently, it is considered that the high resistivity zones extracted by this survey contain few amounts of graphite and IP response is little affected in these zones. Thus, the IP method is available for these high resistivity zones in order to delineate prospective parts.

Since the CSAMT method is not much sensitive to high resistivity and this measurement was carried out with the potential electrode spacing of 100 m, the resistivity distribution related to the mineralization was not able to determine with sufficient accuracy. From this standpoint also, it is significant to carry out the IP method sensitive to high resistivity with high density.

The result of the integrated interpretation is shown in Fig. 2-2-5.



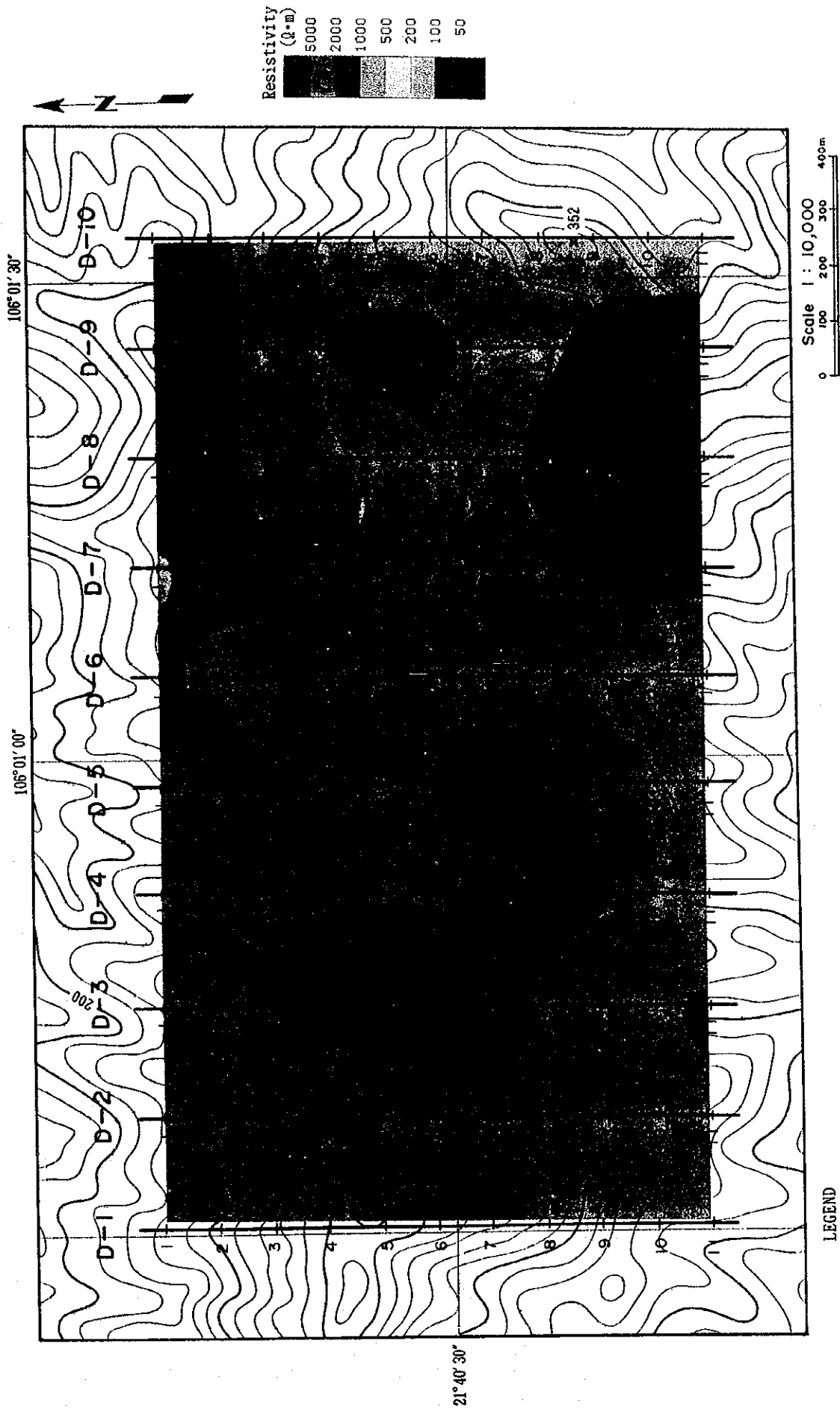


Fig. 2-2-5 Distribution of Geophysical Anomalies (CSAMT Method) in the Da Mai Area (1)

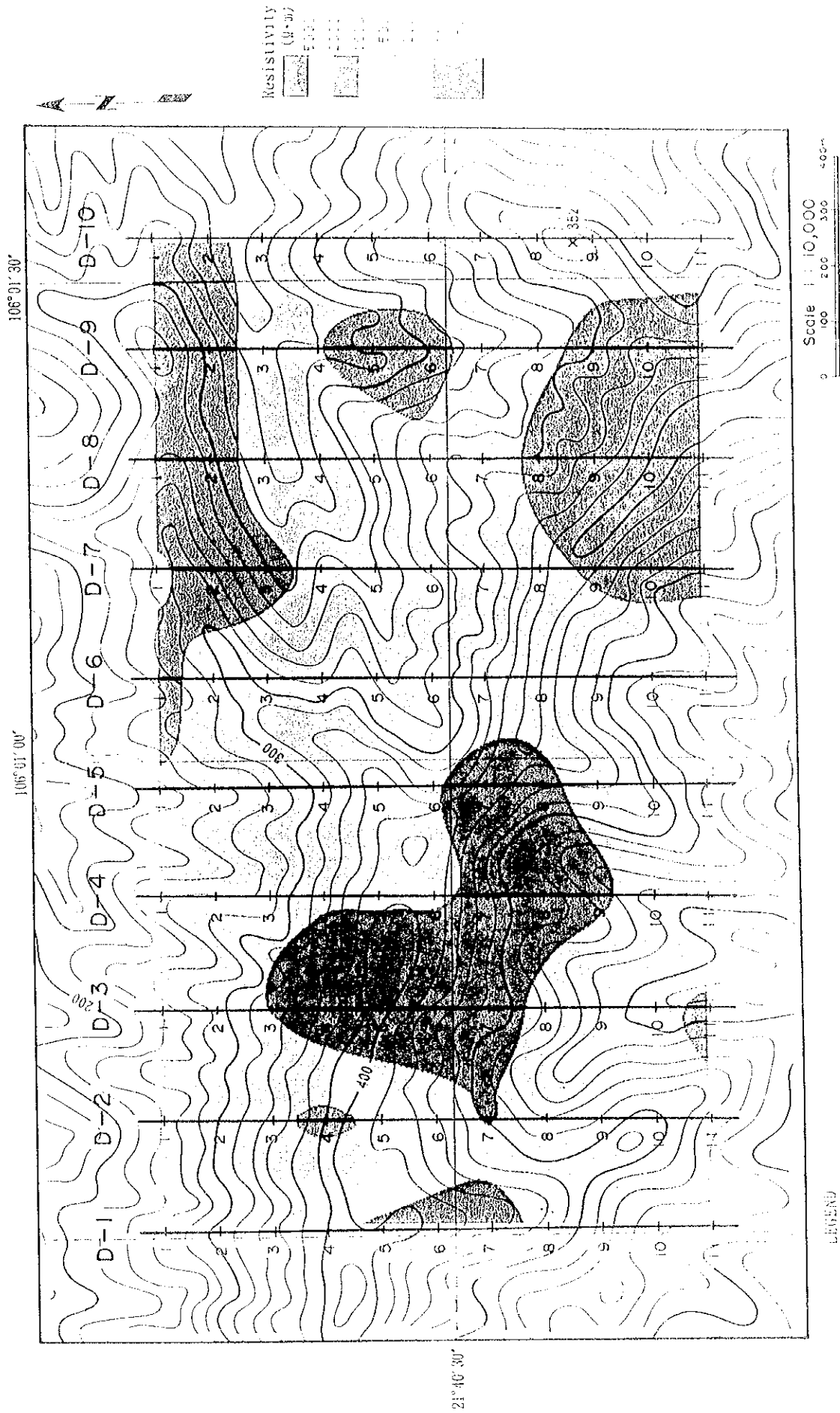


Fig. 2-2-5 Distribution of Geophysical Anomalies (CSAMT Method) in the Da Mai Area (1)



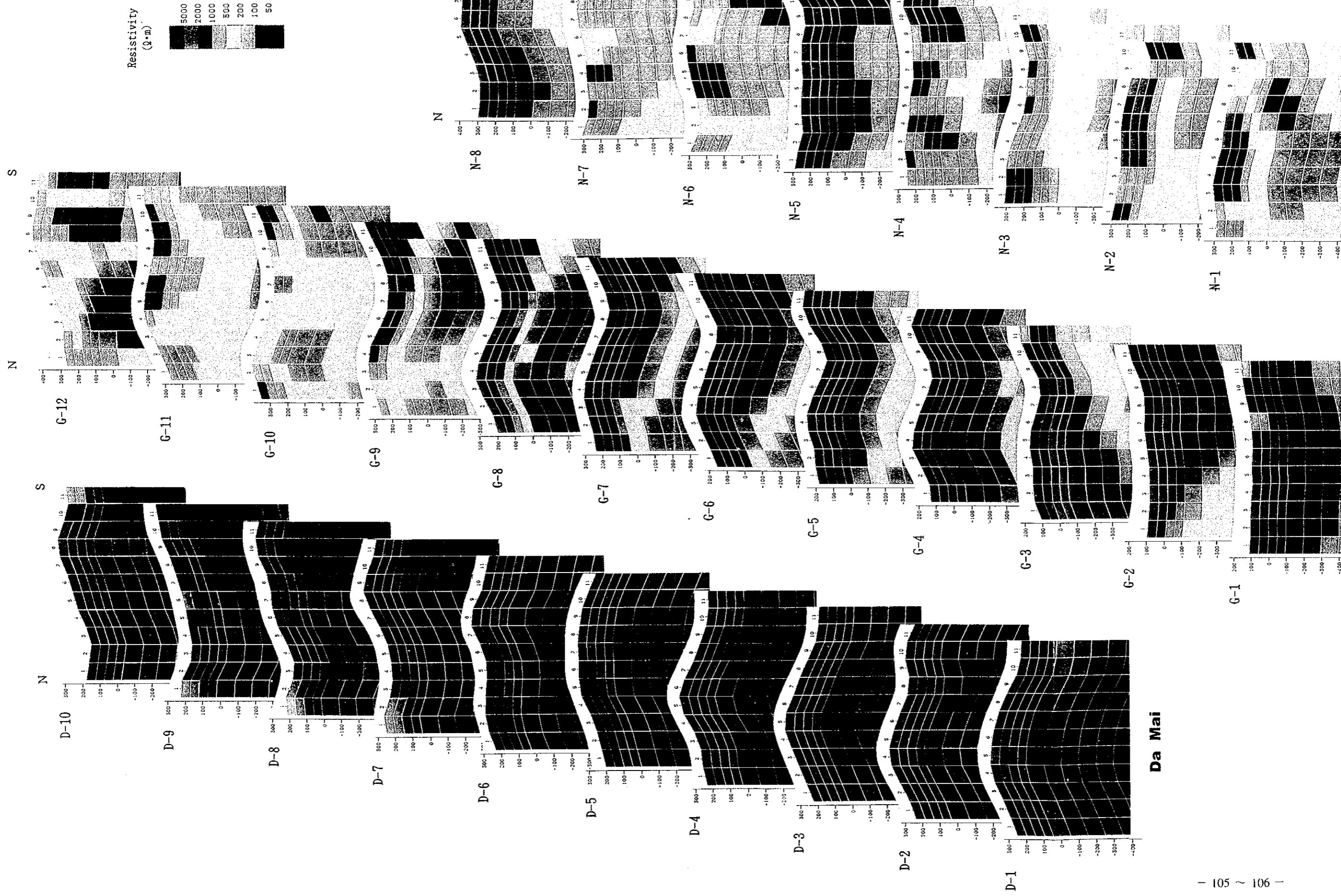


Fig. 2-2-5 Distribution of Geophysical Anomalies (CSAMT Method) in the Da Mai Area (2)

2-5 Geophysical Survey (IP Method)

2-5-1 Outline of Survey

Geophysical survey using Time Domain IP method was carried out in the second phase in the Da Mai and Ngan Me areas. The objectives of the survey were to extract IP anomalies related to mineralization and to investigate the relationship between geophysical and geologic structure in the survey area. These results provided a base for the selection of drilling site.

Amounts of geophysical survey were as follows.

	Da Mai Area	Ngan Me Area	Total
•Total length of survey lines	10 km	10 km	20 km
•Survey points	800 points	800 points	1,600 points
•Laboratory test samples			20 pcs

2-5-2 Survey Method

(1) Methodology

The IP method is the exploration method to observe electric polarization effect (IP effect) in the earth. The IP effect is caused by the following phenomena.

When direct current flows through the rocks containing metallic minerals, electric potential difference is generated between the surface of metallic minerals and pore water around it. This electric potential causes a store of electric charge and induces electric polarization. The electric charge is discharged gradually after current is cut off. It forms the residual voltage decaying with the passage of time. However, the IP effect occurred not only in the rocks containing metallic minerals, but also in some sedimentary rocks containing graphite or clay.

In the time domain IP method, on and off alternating current in the shape of rectangular wave is generally used as transmitter current. Received voltage is composed of the primary voltage V_p observed during current on and the decay voltage (secondary voltage V_s) observed during current off. Chargeability is calculated with received voltage as index to express quantity of IP effect.

The chargeability M is defined in the following equation. It is the proportion of time integral of secondary voltage to primary voltage. Its unit is mV/V .

$$M = 1/V_p / (t_2 - t_1) \cdot \int_{t_1}^{t_2} V_s dt \quad (3)$$

(2) Field Survey

The survey lines (1 km in length, N-E in direction and 100 m in interval) were laid out as shown in figures in the second phase report.

The specifications of measurement are as follows.

Electrode configuration	: Dipole-dipole array
Interval of measuring points	: 50 m
Electrode separation index	: 1 to 5
Electrode spacing	: 50 m
Observed quantity	: Electric potential and chargeability
ON/OFF time	: 2 s
Time at the beginning of Vs measurement	: 500 s
Time at the end of Vs measurement	: 1,050 s

The equipment used in this survey are shown in tables in the second phase report.

(3) Laboratory Test

Resistivity and chargeability of rock samples in the survey areas were measured in laboratory. The same method as in the field measurement was applied. Twenty samples were measured in laboratory.

(4) Analytical Method

The analysis was carried out according to the flow chart as shown in a figure in the second phase report.

Apparent Resistivity Pseudosection: In this section, apparent resistivity was plotted at the depth of $a(n+1)/2$ just under the middle point of the used electrodes for each line.

Apparent Resistivity Map: In this map, the apparent resistivity of the specific electrode separation index was plotted.

Apparent Chargeability Pseudosection: In this section, apparent chargeability was plotted at the depth of $a(n+1)/2$ just under the middle point of the used electrodes for each line.

Apparent Chargeability Map: In this map, the apparent chargeability of the specific electrode separation index was plotted.

2-D Inversion: This analysis assumes that structure is two dimensional, and determines the optimum resistivity distribution of two dimensional model for each line. The distribution of apparent resistivity calculated for the optimum model was best matched to that of the observed apparent resistivity. The finite element method was applied to the forward analysis, and the non-linear least squares method with smoothness constraint was applied to the optimization of resistivity distribution.

After resistivity distribution was obtained, chargeability distribution was determined with the least squares method on the assumption that a observed chargeability was weighted average value of chargeability using the sensitivities of apparent resistivity as a weighting function.

Resistivity Section: In this section, the resistivity distribution below each line was drawn using the results of the 2-D inversion.

Resistivity Map: In this map, the resistivity distribution at the specific level was drawn using the results of the 2-D inversion.

Chargeability Section: In this section, the chargeability distribution below each line was drawn using the results of the 2-D inversion.

Chargeability Map: In this map, the chargeability distribution at the specific level was drawn using the results of the 2-D inversion.

Integrated Interpretation Map: In this map, the geophysical results were integrated with the geologic information.

2-5-3 Results of Field Survey

(1) Observed Data

1) Apparent Resistivity

The pseudosections of the apparent resistivity of every line are shown in figures in the second phase report and the maps of the apparent resistivity of $n=1, 3$ and 5 are shown in figures in the second phase report. The apparent resistivity in the Da Mai area was 316 to $1,000$ ohm-m, and its distribution was little changeful, on the whole. The mean value was about 500 ohm-m. As was seen on the maps, the apparent resistivity showed a tendency to be higher in the deeper zone. In the map of $n=5$, all high resistivity areas more than $1,000$ ohm-m emerged in the ridge parts. It seems to be due to the topographic effect.

2) Apparent Chargeability

The pseudosections of the apparent chargeability of every line are shown in figures in the second phase report and the maps of the apparent resistivity of $n=1, 3$ and 5 are shown in figures in the second phase report. The apparent chargeability in the Da Mai area was mostly lower than 10 mV/V and therefore the background value of chargeability in this area seemed to be lower than 10 mV/V. The strong chargeability anomaly area more than 30 mV/V was detected in the northern part of lines D-IP-8 to D-IP-10. This area showed a tendency to be higher in the deeper zone. The weak chargeability anomaly area was detected in the south of this strong anomaly. This weak anomaly area disappeared in the deep zone.

(2) Analytic Results (2-D Inversion)

1) Resistivity

The resistivity sections drawn with the 2-D inversion are shown in figures in the second phase report. The resistivity maps of 3 levels (SL 250 m, SL 200 m and SL 150 m) are shown in figures in the second phase report. The resistivity in the Da Mai area is higher than 316 ohm-m and changes gently, as a whole. It shows a tendency to be higher in the deeper zone. In the map of SL 150m, high resistivity more than $1,000$ ohm-m is distributed broadly. These tendencies are similar to the results of CSAMT method carried out on the first phase survey.

2) Chargeability

The chargeability sections drawn with the 2-D inversion are shown in figures in the second phase report. The chargeability maps of 3 levels (SL 250 m, SL 200 m and SL 150 m) are shown in figures in the second phase report. The chargeability in the Da Mai area was mostly lower than 10 mV/V and therefore the background value of chargeability in this area was lower than 10 mV/V.

The strong chargeability anomaly zone more than 30 mV/V were extracted in the northern part of lines D-IP-8 to D-IP-10. This anomaly zone has a WNW-ESE direction and is composed of two parallel anomalies, as shown in the map of SL 200m. This anomaly zone tended to continue further to the east of the survey area and extended to the deeper zone. Besides, the weak anomaly zone more than 15 mV/V was extracted in the central part of survey area. This anomaly zone has a WNW-ESE direction, also. However, it tends not to extend the deeper zone.

The resistivity value in the strong chargeability anomaly zone was 316 to 1,000 ohm-m, on the whole. This value was the background resistivity of the Da Mai area. The distinctive relationship between resistivity and chargeability was not found out in this area.

2-5-4 Laboratory Test

The results of the laboratory test are shown in a table in the second phase report. The mean values of resistivity and chargeability for each rock including the samples measured on the first phase are as follows.

Rock	Resistivity (ohm-m)	Chargeability (mV/V)
Quartz Vein	16,919	25.9
Claystone, Siltstone	646	3.9
Shale	1,389	9.8
Sandstone	2,602	13.6
Phyllite	1,726	12.1
Schists	1,716	12.1
Granite	1,734	13.5

The mean value of the resistivity of the rock samples were higher than 1,000 ohm-m except claystone and siltstone. Especially, the resistivity of the quartz vein was remarkably higher (more than 10,000 ohm-m) than that of the other rocks. However, the resistivity of the quartz vein varied widely, depending on the condition of fissures and the content of sulfide minerals (mainly pyrite). The samples containing remarkable fissures measured lower value of about 2,000 ohm-m. Furthermore, as the content of sulfide minerals increased, the resistivity of quartz vein showed a tendency to be lower. The sandstone of the host rock had the second highest resistivity. Especially, quartzitic sandstone (MJVB-

1 core) exhibited high resistivity more than 5,000 ohm-m. Claystone and siltstone were the lowest (about 600 ohm-m) of the rocks in the survey areas. A low resistivity of about 200 ohm-m existed in the shale and schist.

The chargeability of the quartz vein showed the highest value. However, it was clear that its value was correlated with the content of sulfide minerals (mainly pyrite). The samples containing no pyrite measured extremely low less than several mV/V, while a sample containing pyrite measured the largest of 96 mV/V. Relatively high chargeability of about 20 mV/V existed in the phyllite, schist and sandstone. In the case of containing no sulfide mineral, the rocks of the survey areas seemed to be from a few mV/V to 20 mV/V. The drilling core samples measured extremely low chargeability less than several mV/V except quartz vein. It was in line with the low background value of the chargeability in the Da Mai area.

The characteristic relationship between resistivity and chargeability was not found out, except for the quartz vein.

2-5-5 Integrated Interpretation

(1) Relationship between Resistivity and Mineralization

The analytic results, laboratory test results and geologic information led to the following relationship between resistivity and mineralization in the survey areas.

The quartz vein is extremely high (more than 10,000 ohm-m) in resistivity. However, it is very difficult to extract a narrow quartz vein in width by this measurement system. In case where a group of quartz veins is large in size, it is possible to extract a high resistivity zone related to quartz veins.

The development of fractures and content of sulfide minerals lower the resistivity of a zone where quartz veins are distributed, as shown in the laboratory test results. In many cases, small quartz veins contribute to increasing the resistivity obtained by this measurement system. Therefore, the resistivity of a zone where quartz veins are distributed seems to be almost the same as or higher than in the host rock, that is, from medium to high in the survey areas.

(2) Relationship between Chargeability and Mineralization

The analytic results, laboratory test results and geologic information led to the following the relationship between chargeability and mineralization in the survey areas.

In the survey areas, sulfide minerals (mainly pyrite) and graphite are assumed to cause chargeability anomalies. From a geological viewpoint, the rocks in the survey areas contain few amounts of graphite. Therefore, chargeability anomalies result from sulfide minerals (mainly pyrite) accompanying quartz veins. The laboratory test results show that the chargeability value is obviously correlated with the content of sulfide minerals (mainly pyrite).

In the survey areas, it follows from these that a strong chargeability anomaly zone is connected with the zone where quartz veins containing a considerable amount of sulfide minerals are distributed. In case where the chargeability of the host rocks is low, there is a high possibility that a weak chargeability anomaly is the zone where quartz veins containing a small amount of sulfide minerals are distributed.

(3) Relationship between Geophysical Anomaly and Mineralization

In the survey areas, the above discussion gives the followings to the IP anomalies extracted in a zone where quartz veins are distributed.

- Strong chargeability anomaly
- Weak chargeability anomaly
- High resistivity anomaly

Strong chargeability anomaly is highly related to a distribution of quartz veins and connected with a distribution of quartz veins containing a considerable amount of sulfide minerals. Weak chargeability anomaly is expected that quartz veins containing a small amount of sulfide minerals are distributed, in case where the chargeability of the host rocks is low. High resistivity anomaly may be expected that a large group of quartz veins is distributed.

In the following, the relationship between these anomalies extracted in the Da Mai area and the known prospects are discussed.

The distributions of the strong chargeability anomaly zone, weak chargeability anomaly zone and known quartz veins were shown in a figure in the second phase report. The strong chargeability anomaly was regarded as more than 30 mV/V. The weak chargeability anomaly was regarded as more than 15 mV/V, since the background value in the Da Mai area is more than 10 mV/V. These anomaly zones were plotted with the chargeability maps of 3 levels (SL 250 m, SL 200 m and SL 150 m). The high resistivity zone was not done, because the resistivity distribution is little changeful and there is no characteristic anomaly in the Da Mai area. The locations and features of anomaly zones, and the relation to the known prospects are as follows.

Strong Chargeability Anomaly

- Northern part of lines D-IP-8 to D-IP-10

This anomaly zone has a WNW-ESE direction and is composed of two parallel anomalies. It tends to further continue to the east of the survey area and extend to the deeper zone. It seems to reflect the prospect around Khe Dui stream. It suggests that the prospect around the Khe Dui stream

contains a large amount of sulfide minerals and continues to the east.

Weak Chargeability Anomaly

- Central part of the survey area

This anomaly zone has a WNW-ESE. However, it tends not to extend to the deeper zone. It seems to be attributed to the prospect around the Da Mai stream. In this year, the drilling exploration was carried out in the western part of this anomaly zone and caught the groups of quartz veins containing a small amount of sulfide minerals. This result is matched with the geophysical survey results.

(4) Relations to Geologic Structure

In the Da Mai area, the resistivity distribution is little changeable. The geophysical survey results suggest that there are few geologic structures such as fracture zone inducing change of resistivity in the Da Mai area.

The chargeability distribution in these areas tends not to be related to the geologic structure specifically, except for the distribution of quartz veins.

The result of the integrated interpretation is shown in Fig. 2-2-6.

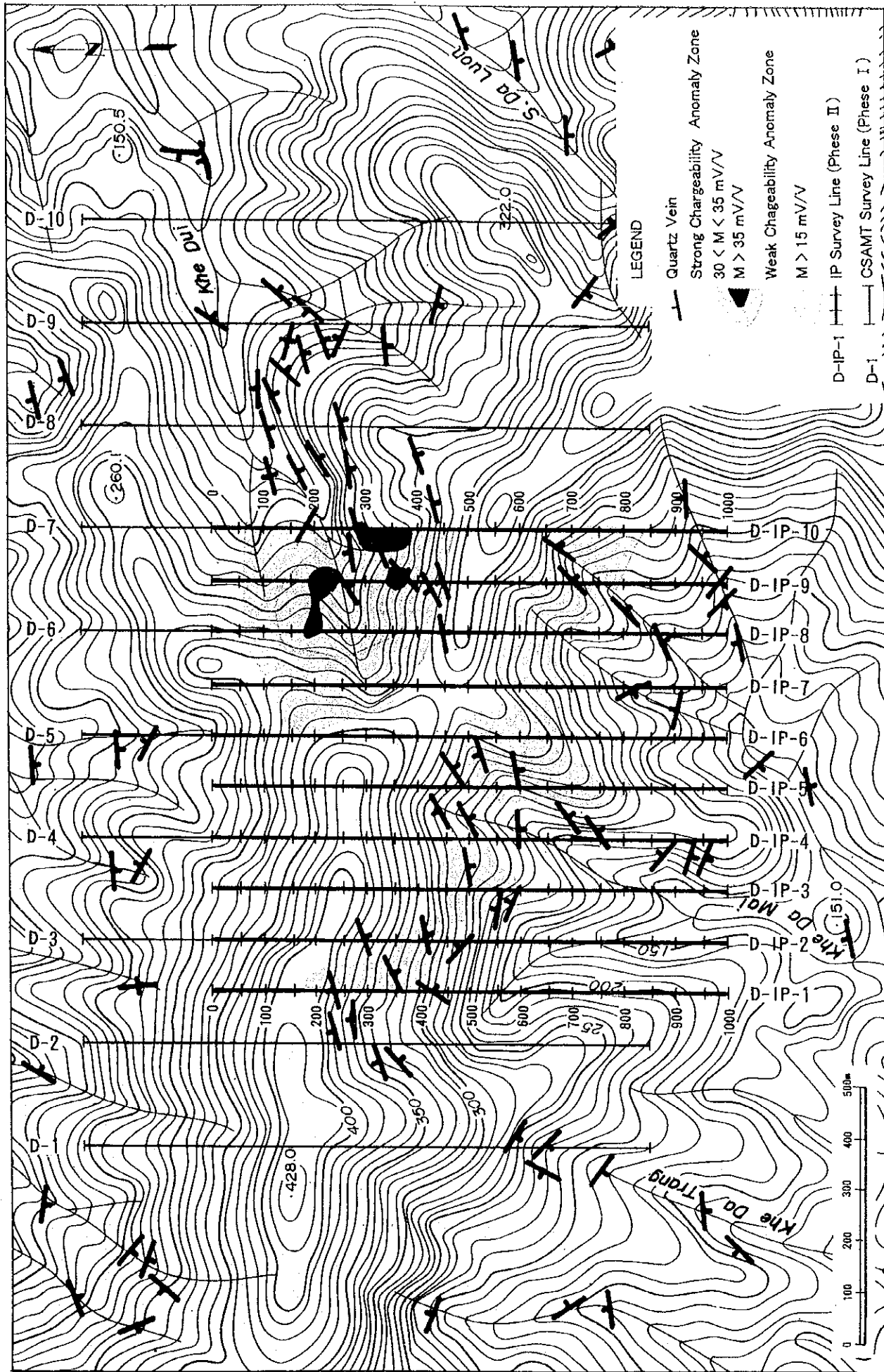
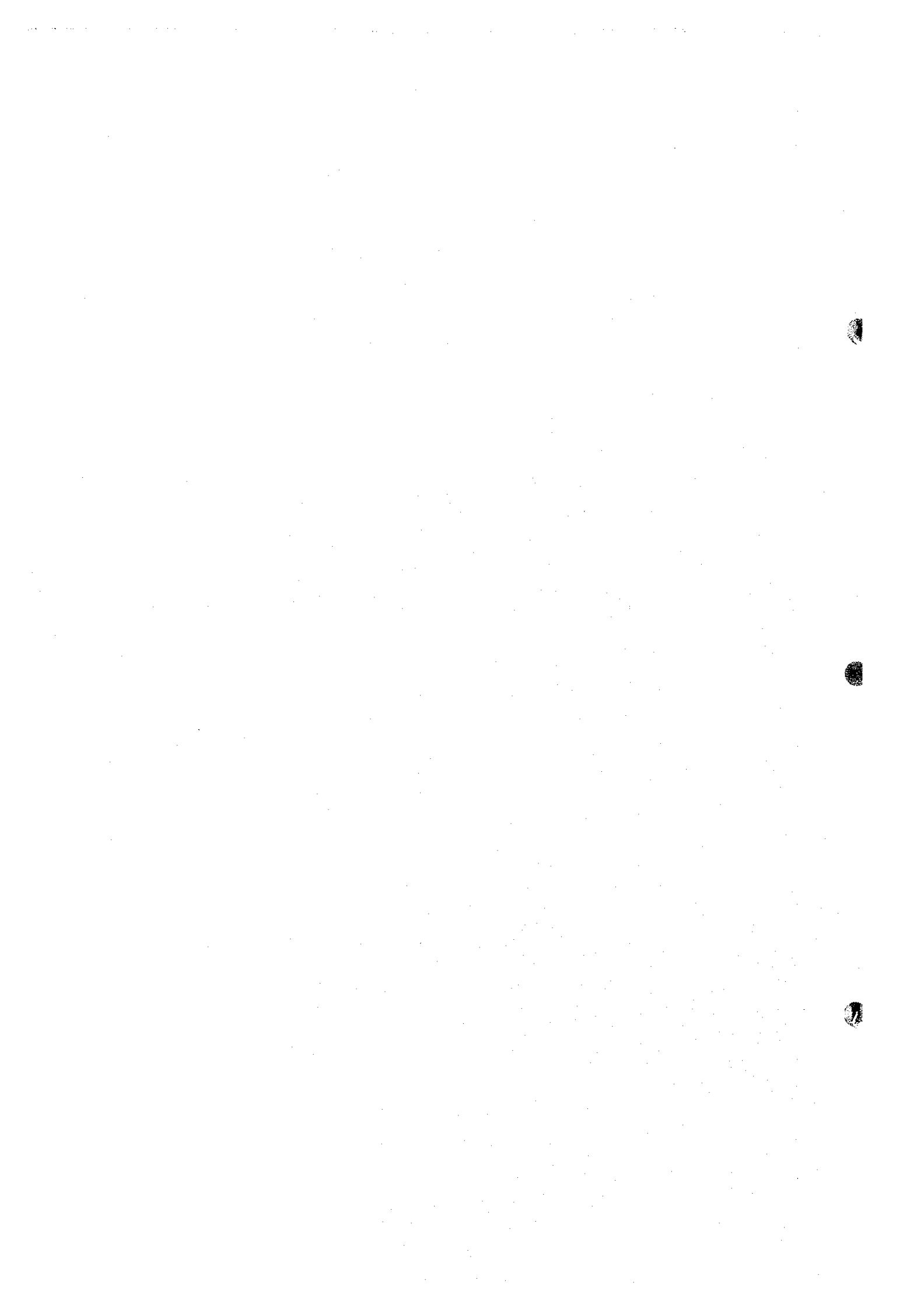


Fig. 2-2-6 Distribution of Geophysical Anomalies (IP Method) in the Da Mai Area



2-6 Drilling (Phase II)

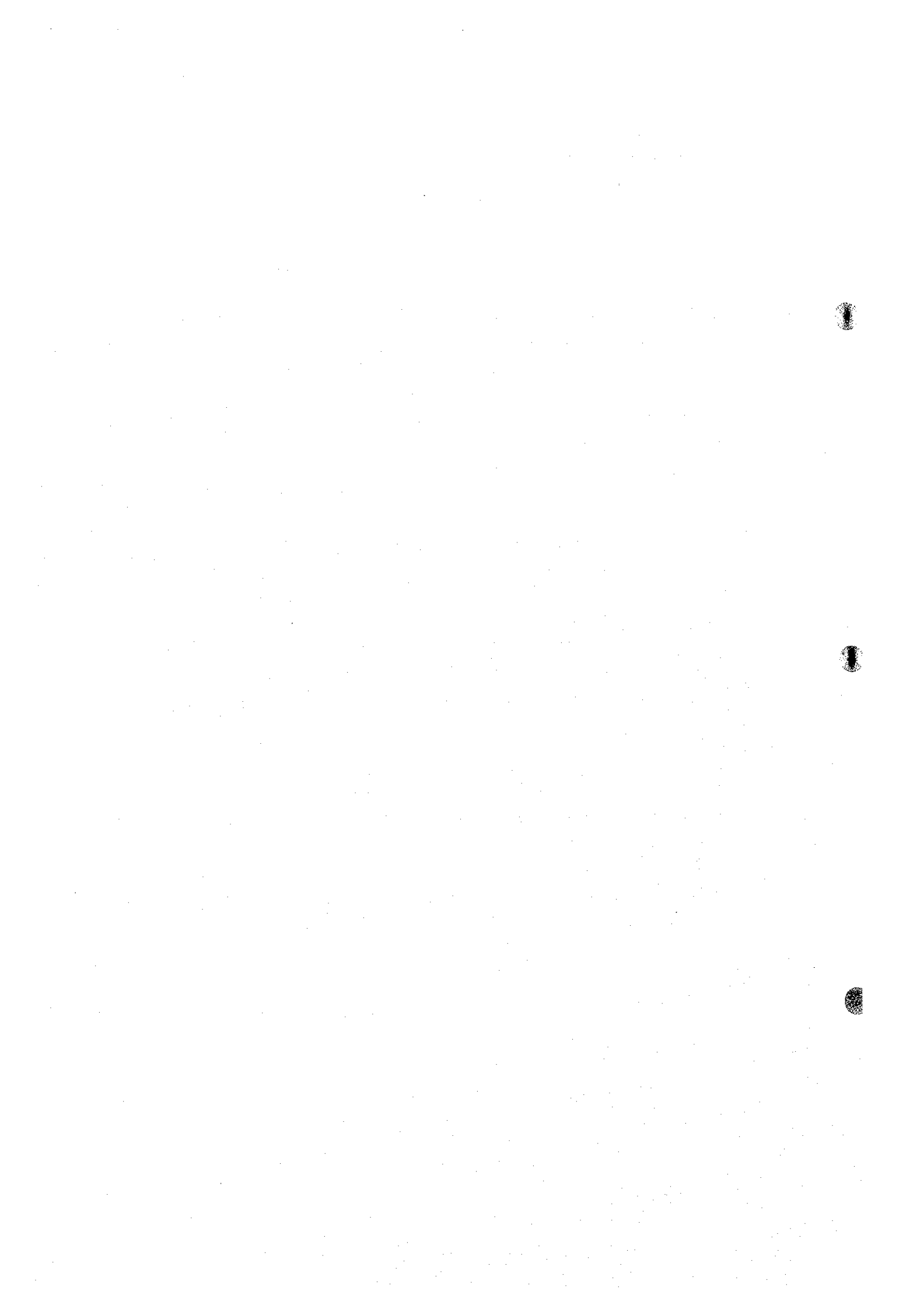
2-6-1 Outline of Drilling

In the second phase, a reconnaissance diamond drilling program comprising two holes totaling 600 m was planned in the Da Mai area. These holes were directed towards the significant geological/geochemical and geophysical anomalous zones. Significant gold mineralized zones at the Da Mai- Khe Dui prospect, which were defined by geological/geochemical and IP geophysical surveys were targeted by two holes -- MJVB-1 and 2.

The drilling program was composed of two inclined holes of 300 m deep each. Target depths were set at 50 to 250 m from the surface. Two holes of 600.00 m in total length have been drilled in this phase. Details of each hole are summarized in the table below. The location map of drill holes is shown in Fig. 2-2-7.

Hole No.	Area & Prospect	Location	Latitude (N)	Longitude (E)	Elevation (m)	Azimuth	Inclination (°)	Length (m)
MJVB-1	Da Mai-Khe Dui (Da Mai Area)	Da Mai Creek	21°40'28" "	106°00'36"	210	N	-45	300.00
MJVB-2	Ditto	W-DaMai Creek	21°40'36" "	106°00'25"	300	N	-45	300.00
Total	2 holes							600.00

A series of drill logs of 1:200 scale was prepared, and the whole drill cores were photographed in color. Fifty-three samples for ore assay were obtained. Six elements (Au, Ag, Cu, Pb, Zn and Fe) were analyzed for ore assay. Twelve polished sections for ore microscopy and ten thin sections for petrography were produced from the cores. Twenty altered rock and quartz samples were examined for X-ray powder diffraction analysis. Ten quartz samples were provided for fluid inclusion studies.



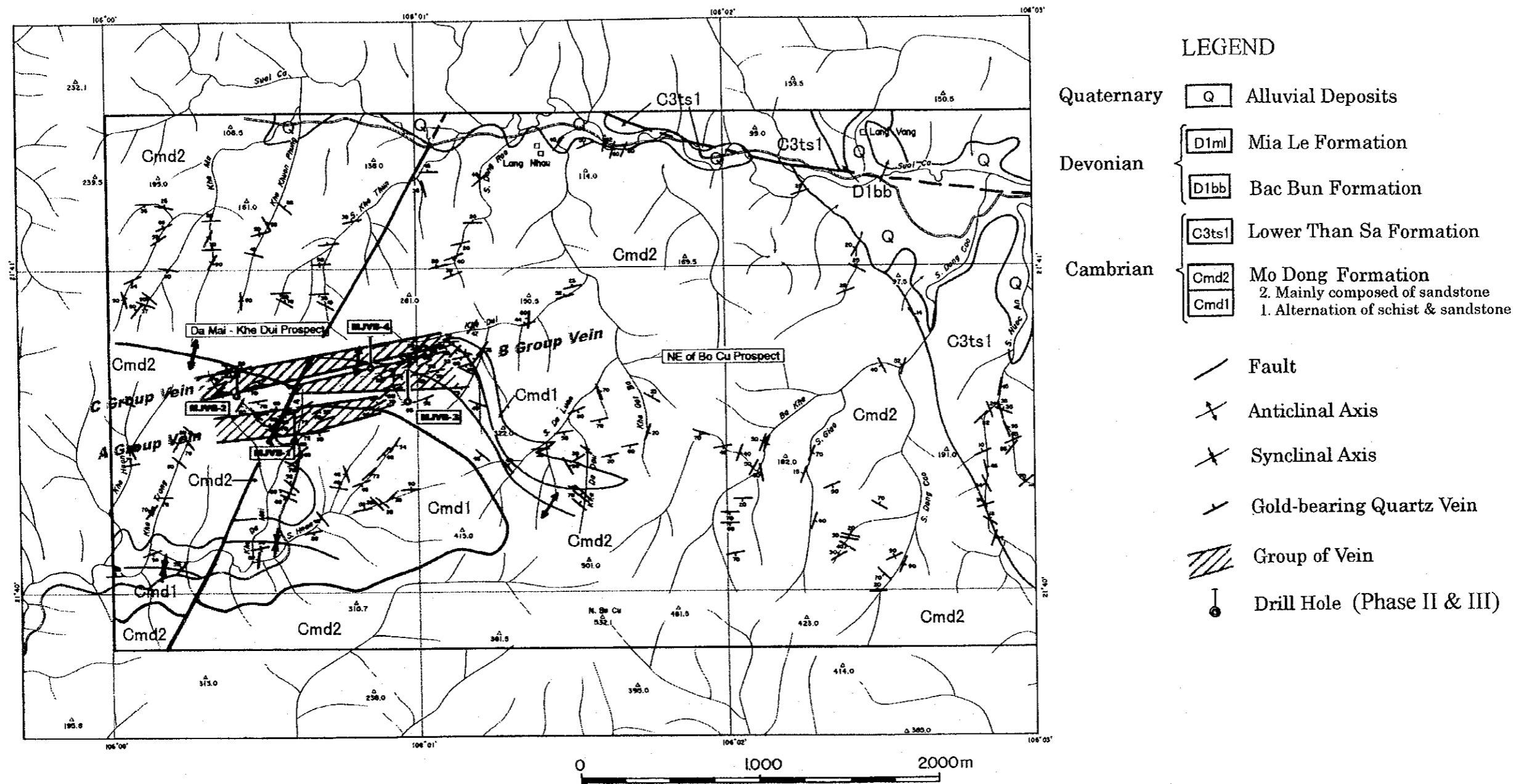


Fig. 2-2-7 Location Map of Drill Holes in the Da Mai Area

2-6-2 Method, Equipment and Progress

(1) Method and Equipment

Method

For the near-surface weathered zone (2 to 4 m), drilling was done by PQ size metal bit (132 mm in diameter) with inserting of PW drive pipes. Weak-weathered bedrock and the upper part of bedrock zone (down to 100 to 150 m) were drilled by the conventional drilling method using HQ size diamond bit (91 mm in diameter). The weak-weathered bedrock continued to 20 to 30 m deep. Reaming at 117 mm in diameter was done by using diamond or metal bit, and HW casing pipes (108 mm in inner diameter) were inserted in this zone. For the upper part of bedrock zone, NW casing pipes (89 mm in inner diameter) were inserted down to approximately 100/150 m. From 100/150 m to 300 m (the end of hole), drilling was made with NQ size diamond bit (76 mm in diameter) and NQ-WL core tube. Bentonite clay, polymer (CMC) and NaOH (pH adjustment agent) were usually mixed in the circulating drilling water. When the water was lost in the hole where fractures were developed, a natural fibrous material (commercial name is GPC made in China) was injected to recover the trouble.

Equipment

Two sets of Russian ZIF-650M drilling machines and two sets of Russian NB-3 drilling pumps were brought into operation in this exploration. Drill rigs were Vietnamese domestic made tripod-type angled ones. Specifications of drilling machine and equipment are shown in Table 2-2-4.

Working System

Drilling operation was carried out by three shifts per day (8 hours per shift), while the appurtenant works, such as rig construction, mobilization and demobilization, were done by one shift per day (8 to 10 hours). A shift crew consisted of one drilling engineer and three to four workers normally. Additional twenty workers (round figures) were involved in case of the appurtenant work. A series of base camps for drilling operation were built at the foot of Da Mai creek.

Transportation

The drilling machine and equipment were transported to the Da Mai area by a convoy of 7-ton trucks and 5-ton trucks. A couple of 4-WD trucks (2 to 5 tons in capacity) and a bulldozer were

chartered for the transportation of drilling machine and equipment from the main road to the drilling sites through a series of roads which was constructed for this drilling purpose for about 2 km.

Supply for the camp was made once in a week. Fuel and foods were bought at Thai Nguyen, and were transported by chartered cars.

Drilling Water

Water for drilling was pumped up from the middle reaches of Da Mai creek to the drilling sites via pipelines whose length was about 2 km in total. The difference of altitudes between pumping station to the drilling sites was nearly 200 m. Mud water was also prepared in that pumping station, and sent through the pipeline to the drilling sites.

Withdrawal

After the completion of drilling program, the machine and equipment were withdrawn by trucks through the same route to Hanoi. The drill holes were capped, and drilling sites were cleaned and reclaimed. The drilling cores, of which the half was taken for assay samples in some part, were kept in the storage house in the office of Division NE of DGMV, Thai Nguyen.

(2) Progress of Drilling

The progress of each drill hole is described below.

MJVB-1: For the near-surface weathered zone (2.40 m), drilling was done by PQ size metal bit (132 mm in diameter) with inserting of drive pipes (146 mm in inner diameter). Weak-weathered bedrock and the upper part of bedrock zone (down to 150 m) were drilled by the conventional drilling method using HQ size diamond bit (91 mm in diameter) for the maximum core recovery. The weak-weathered bedrock continued to 17 m deep. Circulating water escaped from the hole at 6 m through cracks. Reaming at 117 mm in diameter was done by using diamond and metal bits, and HW casing pipes (108 mm in inner diameter) were inserted in this zone. For the upper part of bedrock zone, NW casing pipes (89 mm in inner diameter) were inserted down to 150 m.

From 150 m to 300 m (the end of hole), drilling was made with NQ size diamond bit (76 mm in diameter) and NQ-WL core tube. However, in some part of the drill hole where was made up of very hard rocks comparatively easy to be broken in a wedge-shaped fragment, the drilling method was switched into the conventional one for the requirement of core recovery.

Bentonite clay, polymer (CMC) and NaOH (pH adjustment agent) were usually mixed in the circulating drilling water. The drilling water was lost in the hole at 270 m where fractures were developed.

Drill hole survey was made using a Toropali survey instrument. The results of survey for inclination were: -45° at 0 m and 100 m, -41° at 200 m, and -32° at 300 m. The recovery of cores was 98 % in total because of careful drilling operation.

MJVB-2: For the near-surface weathered zone (2.50 m), drilling was done by PQ size metal bit (132 mm in diameter) with inserting of drive pipes (146 mm in inner diameter). Weak-weathered bedrock and the upper part of bedrock zone (down to 106.85 m) were drilled by the conventional drilling method using HQ size diamond bit (91 mm in diameter) for the maximum core recovery. The weak-weathered bedrock continued to 30 m deep. Circulating water escaped from the hole at around 18 m through cracks. Reaming at 117 mm in diameter was done by using diamond and metal bits, and HW casing pipes (108 mm in inner diameter) were inserted in this zone. For the upper part of bedrock zone, NW casing pipes (89 mm in inner diameter) were inserted down to 106.85 m.

From 106.85 m to 300 m (the end of hole), drilling was made with NQ size diamond bit (76 mm in diameter) and NQ-WL core tube. However, in some part of the drill hole where was made up of very hard rocks and quartz vein zones, the drilling method was switched into the conventional one to keep the core recovery in a certain level.

Bentonite clay, polymer (CMC) and NaOH were usually mixed in the circulating drilling water. The drilling water was lost in the hole at 60.50, 160.00 and 283.50 m where fractures were developed. GPC (Telstop) was added to the mud water to prevent the water loss.

Drill hole survey was made using a Toropali survey instrument. The results of survey for inclination were: -45° at 0 m, -42° at 100 m, -38° at 200 m, and -35° at 300 m. The overall core recovery was 99 % in this hole.

2-6-3 Geologic Description of Drill Holes

The geology of the area where drilling exploration was carried out in the second phase is composed of schist and sandstone of the Mo Dong Formation.

Weathered schist and sandstone occur below the surface soil (a few to 30 cm thick), and extends to nearly 2 to 3 m deep along the drill hole (every hole has drilled at an angle of -45 degrees). Fresh bedrock appears below a few to 30 m in depth. The results of laboratory works and assaying of drill cores are summarized in Table 2-2-5. Drill hole sections are shown in Figs. 2-2-8 and 2-2-9.

MJVB-1: The geology around the drill hole MJVB-1 is composed of schist and sandstone of the Mo Dong Formation. It is located at the upper reaches of Da Mai creek. The altitude of the drill hole is about 210 m above sea level. The purpose of this hole was to investigate the lower extension of gold mineralization in the central part of the Da Mai-Khe Dui prospect. It mainly targeted at the Group A veins in the Da Mai-Khe Dui prospect. The geology of the drill hole is divided into two series: alternation of schist and sandstone (0 to 113.20 m), and sandstone with intercalation of schist layers (113.20 to EOH=300.00 m). The details of geology of the drill hole were described in the second phase report.

MJVB-2: The geology around the drill hole MJVB-2 is composed of schist and sandstone of the Mo Dong Formation. It is located at the upper reaches of West Da Mai creek. The altitude of the drill hole is about 300 m above sea level. The purpose of this hole was to investigate the lower extension of gold mineralization in the western part of the Da Mai-Khe Dui prospect. It mainly targeted at the Group C veins in the DaMai-Khe Dui prospect. The geology of the drill hole is mostly composed of massive sandstone. It partly contains thin layers of schist (0 to 66.50 m and 240.00 to 247.70 m). The details of geology of the drill hole were described in the second phase report.

Table 2-2-5 Summary of Assay Results of Drill Cores (1)

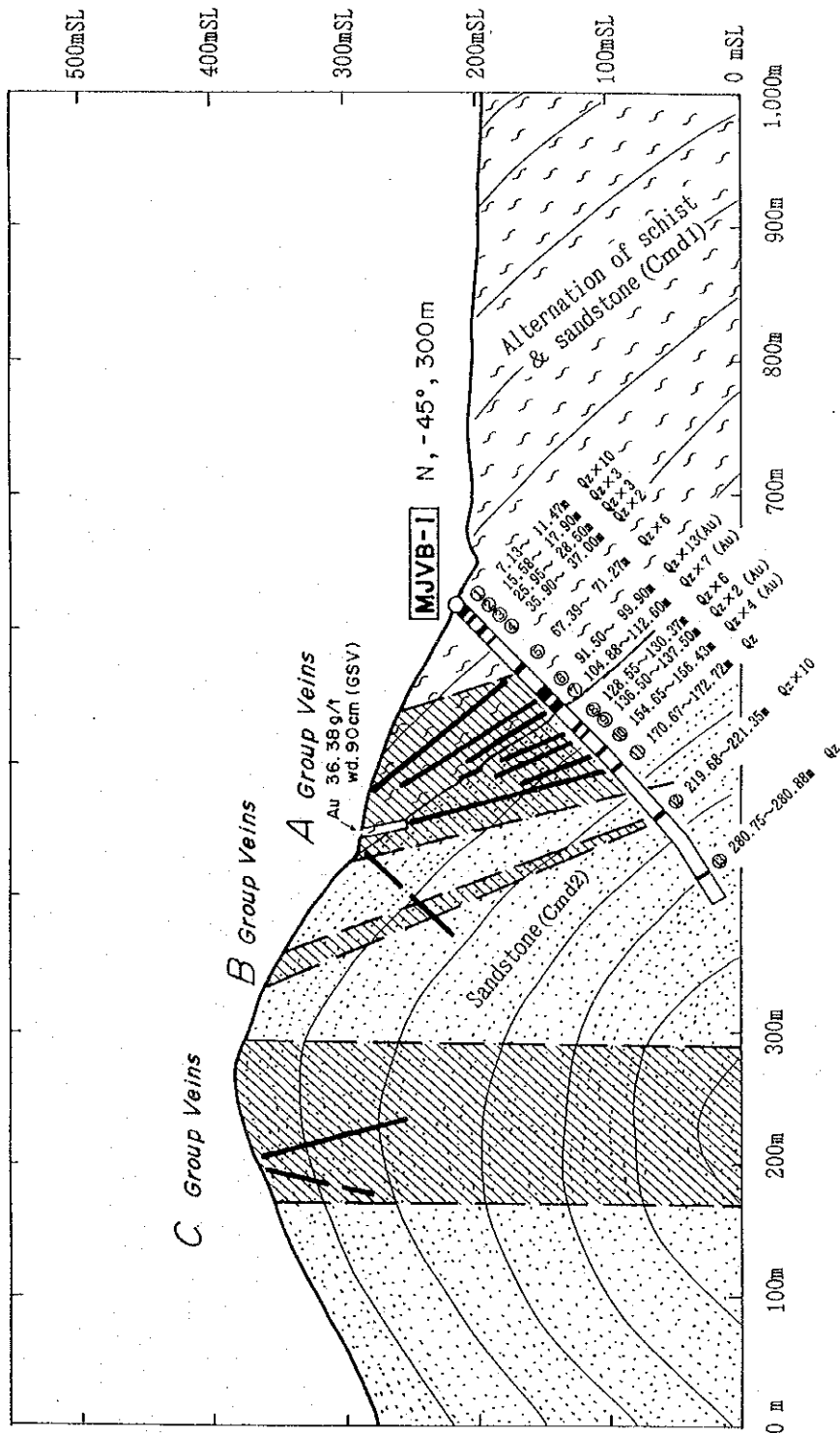
Ser No.	Sample No.	Depth (m)		Sample Width (cm)	Au (g/t)	Ag (g/t)	Cu (%)	Pb (%)	Zn (%)	Fe (%)	Remarks
		From	To								
	MJVB-1										
1	101A	10.60	10.70	10	0.008	<0.5	0.001	<0.001	<0.001	0.30	White partly gray Qz vein, Limo (Py) diss.
2	102A	17.00	17.90	90	0.004	<0.5	0.001	<0.001	0.001	2.06	White Qz netwk zone
3	103A	28.00	28.65	65	0.004	<0.5	0.001	0.001	0.007	4.51	White Qz vein
4	104A	69.10	69.58	48	0.005	<0.5	0.001	<0.001	0.001	3.15	L-gray Qz vein, Py diss.
5	124A	96.00	97.00	100	0.005	<0.5	0.006	0.004	0.004	3.92	White Qz vein/breccia zone
6	105A	97.10	97.85	75	0.010	<0.5	0.001	0.001	0.004	3.10	White Qz vein/breccia, Py diss.
7	106A	98.30	98.94	64	0.008	<0.5	0.002	0.001	0.004	2.82	White Qz vein/breccia, Py diss, visible Au(?)
8	107A	99.00	99.90	90	0.003	<0.5	0.004	0.003	0.004	2.90	White Qz vein/breccia, Py diss.
9	109A	104.88	105.35	47	<0.001	<0.5	0.001	0.002	0.004	3.10	White Qz vein/breccia, Py diss.
10	110A	105.55	105.85	30	<0.001	<0.5	0.002	0.003	0.004	2.95	White Qz vein/breccia, Py diss.
11	112A	106.40	106.80	40	0.002	<0.5	0.001	0.002	0.004	2.85	White Qz vein/breccia, Py diss.
12	113A	107.62	108.40	78	0.004	<0.5	0.001	0.002	0.003	2.90	White Qz vein/breccia, Py diss, visible Au
13	114A	108.58	109.00	42	<0.001	<0.5	0.002	0.004	0.004	3.58	White Qz vein/breccia, Py diss.
14	115A	110.25	110.85	60	<0.001	<0.5	0.001	0.001	0.002	2.15	White partly gray Qz vein/breccia, Py diss.
15	116A	128.55	129.30	75	0.011	<0.5	0.003	0.001	0.005	2.91	White Qz vein/veinlet
16	117A	129.30	130.37	107	0.001	<0.5	0.001	0.005	0.005	3.24	White Qz vein/veinlet
17	118A	136.50	137.00	50	0.002	<0.5	0.013	0.003	0.008	3.60	White Qz vein/veinlet, visible Au.
18	119A	137.00	137.50	50	0.003	<0.5	0.002	0.009	0.003	2.15	White Qz vein/veinlet
19	121A	154.65	155.21	56	0.008	<0.5	0.001	0.001	0.002	2.27	L-gray Qz vein/veinlet, Py diss, visible Au
20	122A	155.28	155.63	35	0.004	<0.5	0.001	<0.001	<0.001	0.99	L-gray Qz vein/veinlet, Py diss.
21	235A	170.67	172.72	205	0.010	<0.5	0.031	0.031	0.051	3.30	White/L-gray Qz vein, Py, As diss.
22	125A	220.00	221.35	135	0.011	<0.5	0.003	0.002	0.006	2.97	White Qz veinlet
23	126A	280.75	280.88	13	0.016	<0.5	0.004	0.003	0.006	2.93	L-gray Qz vein, Py diss.
	MJVB-2										
24	201A	51.24	51.52	28	56.640	9.0	0.009	0.113	0.016	1.88	Gray Qz vein, Limo diss.
25	202A	76.88	77.43	55	0.182	<0.5	0.002	0.001	0.001	2.41	L-gray Qz vein, Py, As diss.
26	203A	81.13	81.33	20	0.440	<0.5	0.015	0.000	0.001	2.78	L-gray Qz vein
27	204A	104.75	104.97	22	0.070	<0.5	0.002	0.001	0.001	2.06	Gray Qz vein
28	205A	118.02	118.62	60	0.140	<0.5	0.001	0.001	0.001	1.32	L-gray Qz vein, Py diss.
29	206A	119.13	119.42	29	0.110	<0.5	0.001	0.001	0.001	1.34	L-gray Qz vein, Py diss.
30	207A	120.81	121.09	28	0.430	<0.5	<0.001	<0.001	0.001	3.26	L-gray Qz network, Py diss.
31	208A	135.00	135.40	40	0.138	<0.5	0.002	0.001	0.001	1.47	L-gray Qz vein/network, Py, As diss.
32	209A	137.38	137.87	49	1.800	2.0	0.012	0.008	0.001	3.10	White/gray Qz vein/network, Py, Cp diss.
33	210A	138.90	139.30	40	0.112	<0.5	0.003	0.001	0.003	3.61	White/gray Qz vein/network, Py, As diss.
34	211A	141.30	141.46	16	0.185	<0.5	0.001	0.001	0.002	2.83	L-gray Qz vein, Py diss.
35	212A	146.45	146.66	21	0.039	1.0	0.003	0.006	0.034	2.64	L-gray Qz vein, Py diss.
36	213A	148.20	149.15	95	0.007	<0.5	0.003	0.001	0.001	1.63	L-gray Qz vein/network, Py, As diss, visible Au
37	214A	149.15	150.00	85	0.011	<0.5	0.001	<0.001	0.001	1.31	L-gray Qz vein/network, Py, As diss.
38	215A	150.00	151.05	105	0.035	<0.5	0.001	<0.001	0.001	2.38	Gray Qz network, Py, As diss.
39	216A	151.05	152.10	105	0.040	<0.5	0.001	<0.001	0.001	1.84	Gray Qz network, Py, As diss, visible Au
40	217A	154.40	155.85	145	0.039	<0.5	0.001	0.002	0.011	2.13	L-gray Qz veinlet
41	218A	159.00	159.60	60	0.067	1.0	0.001	0.005	0.007	3.39	White/L-gray Qz vein, Py diss.
42	241A	181.00	181.11	11	1.020	<0.5	0.009	<0.001	0.013	4.42	Gray Qz veinlet, Py diss.
43	242A	181.11	181.22	11	0.120	<0.5	0.010	0.006	0.021	2.60	Gray Qz veinlet, Py diss.
44	220A	181.22	181.32	10	10.815	<0.5	0.001	0.001	0.002	2.54	Gray Qz veinlet, Py diss, visible Au
45	244A	181.32	181.57	25	0.020	<0.5	0.006	<0.001	0.014	2.42	Gray Qz veinlet
46	245A	181.57	181.80	23	0.050	<0.5	0.005	<0.001	0.010	3.78	Gray Qz veinlet
47	222A	200.20	200.30	10	0.136	<0.5	<0.001	<0.001	0.001	5.57	L-gray Qz veinlet, Py, Po diss.
48	223A	201.35	201.67	32	0.104	<0.5	0.001	<0.001	0.001	4.00	L-gray Qz veinlet, Py, Po diss.
49	224A	207.35	208.20	85	0.055	<0.5	0.118	0.001	0.001	1.86	White/gray Qz vein, Py, As, Cp diss.
50	225A	208.40	209.06	66	0.072	<0.5	0.001	<0.001	0.001	2.69	White/gray Qz vein, Py, As diss.
51	226A	256.67	256.79	12	1.400	<0.5	0.016	0.160	0.031	3.14	Silicified zone with white Qz veinlet, visible Au
52	227A	290.00	290.72	72	0.030	<0.5	0.012	0.006	0.029	2.90	L-gray Qz vein/breccia Py, Cp diss.
53	228A	291.45	292.05	60	0.010	<0.5	0.010	0.008	0.032	2.28	White/L-gray Qz vein, Cp diss.

Table 2-2-5 Summary of Assay Results of Drill Cores (2)

Ser No.	Sample No.	Depth (m)		Sample Width (cm)	Au (g/t)	Ag (g/t)	Cu (%)	Pb (%)	Zn (%)	Fe (%)	Remarks
		From	To								
MJVB-3											
1	301	31.35	31.90	55	0.020	0.6	0.003	<0.001	0.003	6.48	White/L-gray Qz veinlets
2	302	32.22	32.45	23	0.010	<0.5	0.028	0.001	0.004	5.57	White/L-gray Qz veinlets, Py & Lmo dis.
3	325Y	79.23	79.30	7	0.015	0.7	0.002	<0.001	0.007	4.98	White/L-gray Qz veinlet
4	305	79.37	79.50	13	0.020	<0.5	0.003	<0.001	0.005	3.71	White/L-gray Qz vein, Lmo dis.
5	306	79.85	80.20	35	75.600	3.0	0.005	0.001	0.005	3.77	White/L-gray Qz-Calc vein, Py & Lmo dis (s)
6	307	84.97	85.40	43	0.310	<0.5	0.002	0.002	0.001	1.52	L-gray Qz vein, Py & Lmo dis (m)
7	308	103.90	104.08	18	0.030	<0.5	0.001	0.003	0.002	2.14	L-gray Qz vein, Py & Lmo dis (w)
8	310	109.25	110.15	90	0.020	<0.5	0.008	0.002	0.004	3.99	White/L-gray Qz veinlets/netwk zone, Py dis.
9	311	131.70	132.03	33	0.070	<0.5	0.001	0.001	0.004	3.66	White/L-gray Qz-Chl vein, Py & As dis
10	326Y	132.95	133.15	20	0.012	<0.5	0.001	0.001	0.005	5.06	White Qz veinlets, Py diss.
11	312	141.74	141.92	18	0.020	<0.5	0.001	0.018	0.003	2.59	White/L-gray Qz-Cal-Chl vein, Py dis.
12	313	147.60	147.93	33	1.770	<0.5	0.006	0.003	0.010	6.48	L-gray Qz-Cal-Chl netwk zone, Py dis (m)
13	327Y	154.05	154.12	7	0.053	<0.5	0.003	0.006	0.005	4.50	L-gray Qz-Chl vein, Py & As dis (m)
14	314	175.32	175.55	23	0.150	<0.5	0.002	0.009	0.003	1.80	White/L-gray Qz vein, Py & As dis (m)
15	315	180.95	181.08	13	0.020	<0.5	0.005	0.001	0.005	4.56	White Qz vein, Py & As dis (m)
16	328Y	183.00	183.15	15	0.014	<0.5	0.001	0.001	0.005	4.56	White Qz vein
17	316	183.50	183.75	25	0.020	<0.5	0.001	0.001	0.002	1.75	White Qz-Chl vein, Py & As dis (w)
18	318	230.77	231.14	37	0.570	<0.5	0.001	0.001	0.001	3.15	White Qz-Cal-Chl vein, Py & As dis (s)
19	329Y	232.20	232.37	17	<0.001	<0.5	0.004	0.003	0.002	3.55	White/L-gray Qz veinlets
20	319	244.23	244.42	19	0.180	<0.5	0.003	0.001	0.001	2.48	White/L-gray Qz-Cal-Chl vein/netwk zone, Py & As dis (s)
21	320	244.96	245.68	72	0.100	<0.5	0.002	0.002	0.003	4.90	White/L-gray Qz-Cal-Chl vein/netwk zone, Py & As dis (s)
22	330Y	247.10	247.20	10	0.014	<0.5	0.001	<0.001	0.001	1.80	White/L-gray Qz-Cal-Chl vein/netwk zone, Py & As dis (s)
23	321	247.55	248.34	79	0.050	<0.5	0.002	0.001	0.003	4.73	White/L-gray Qz-Cal-Chl vein/netwk zone, Py & As dis (s)
24	331Y	250.10	250.40	30	0.025	<0.5	0.003	0.001	0.005	6.19	White/L-gray Qz-Cal-Chl vein/netwk zone, Py & As dis (s)
25	322	253.40	253.95	55	0.020	1.0	0.003	0.005	0.004	4.34	White/L-gray Qz-Cal-Chl vein/netwk zone, Py & As dis (s)
26	323	273.00	273.15	15	0.020	<0.5	0.001	0.002	0.001	1.52	White Qz vein
MJVB-4											
27	401	38.40	38.80	40	0.020	0.5	0.001	0.005	0.004	2.93	L-gray Qz-Cal vein, Py diss (w)
28	402	40.05	40.37	32	0.010	<0.5	0.002	0.002	0.002	2.59	L-gray Qz-Cal vein, Py diss (w)
29	403	53.93	54.47	54	0.020	<0.5	0.003	0.003	0.007	3.67	White Qz-Cal veinlets, Py diss (m)
30	404	60.15	60.60	45	12.400	0.8	0.005	<0.001	0.007	4.22	White Qz-Cal veinlets, Py, As, Cp dis (m)
31	405	74.45	75.10	65	0.120	<0.5	0.004	0.002	0.008	4.28	White Qz-Cal veinlets, Py & As dis (m)
32	407	102.45	102.94	49	0.110	<0.5	0.001	0.002	0.012	1.86	White Qz-Cal vein, Py diss (spat)
33	409	115.48	115.64	16	0.050	<0.5	0.002	<0.001	0.004	2.31	White Qz-Cal veinlets/netwk zone, Py & As dis (s)
34	410	116.67	117.95	128	0.050	<0.5	0.005	0.001	0.005	4.22	White Qz-Cal veinlets/netwk zone, Py & As dis (s)
35	411	118.55	118.95	40	0.010	<0.5	0.003	0.003	0.002	1.80	White Qz-Cal veinlets/netwk zone, Py & As dis (s), Partly Chl
36	430Y	119.08	119.60	52	0.012	<0.5	0.007	0.004	0.011	5.01	White Qz-Cal veinlets/netwk zone, Py & As dis (s), Partly Chl
37	412	126.25	127.30	105	0.020	<0.5	0.003	<0.001	0.004	2.36	White Qz-Cal veinlets/netwk zone, Py & As dis (s)
38	413	131.65	132.10	45	0.060	<0.5	0.005	0.002	0.005	5.06	White Qz-Cal veinlets/netwk zone, Py & As dis (s)
39	415	143.40	143.75	35	0.020	<0.5	0.002	<0.001	0.005	2.59	White Qz-Cal veinlets/netwk zone, Py & As dis (s)
40	416	145.40	145.50	10	0.010	0.5	0.004	0.001	0.008	4.22	White Qz-Cal veinlets/netwk zone, Py & As dis (s)
41	417	145.53	145.88	35	0.020	<0.5	0.004	0.002	0.004	3.10	White Qz-Cal veinlets/netwk zone, Py & As dis (s)
42	418	146.00	146.65	65	0.010	<0.5	0.003	0.001	0.003	2.59	White Qz-Cal veinlets/netwk zone, Py & As dis (s)
43	419	147.00	147.55	55	0.010	<0.5	0.002	0.001	0.003	1.07	White Qz-Cal veinlets/netwk zone, Py & As dis partly
44	420	148.10	149.08	98	0.010	<0.5	0.003	0.002	0.007	3.10	White Qz-Cal veinlets/netwk zone, Py & As dis (m)
45	421	153.04	153.53	49	0.200	<0.5	0.004	0.001	0.007	3.88	White Qz-Chl veinlet/netwk zone
46	422	153.65	153.75	10	0.020	<0.5	0.004	0.001	0.007	3.82	White Qz-Cal veinlets/netwk zone, Py & As dis (s)
47	423	153.90	153.98	8	0.020	<0.5	0.001	0.003	0.006	3.27	White Qz-Cal veinlets/netwk zone, Py & As dis (s)
48	424	157.70	158.03	33	0.010	<0.5	0.003	0.001	0.004	2.14	White Qz-Cal veinlets/netwk zone, Py & As dis (m)
49	425	161.23	161.40	17	0.020	<0.5	0.003	0.008	0.008	2.64	White Qz-Cal veinlets/netwk zone, Py & As dis (s)
50	426	192.80	193.20	40	0.010	<0.5	0.001	0.002	0.004	1.24	Black/white banded Qz vein, Py diss (s)
51	428	254.00	254.45	45	0.010	<0.5	0.002	0.001	0.002	2.36	Sil/clayey zone with Qz veinlets
52	429	256.29	256.40	11	0.120	<0.5	0.001	0.015	0.001	0.96	L-gray Qz-Cal vein, Py & Gs dis (w)

Table 2-2-5 Summary of Assay Results of Drill Cores (3)

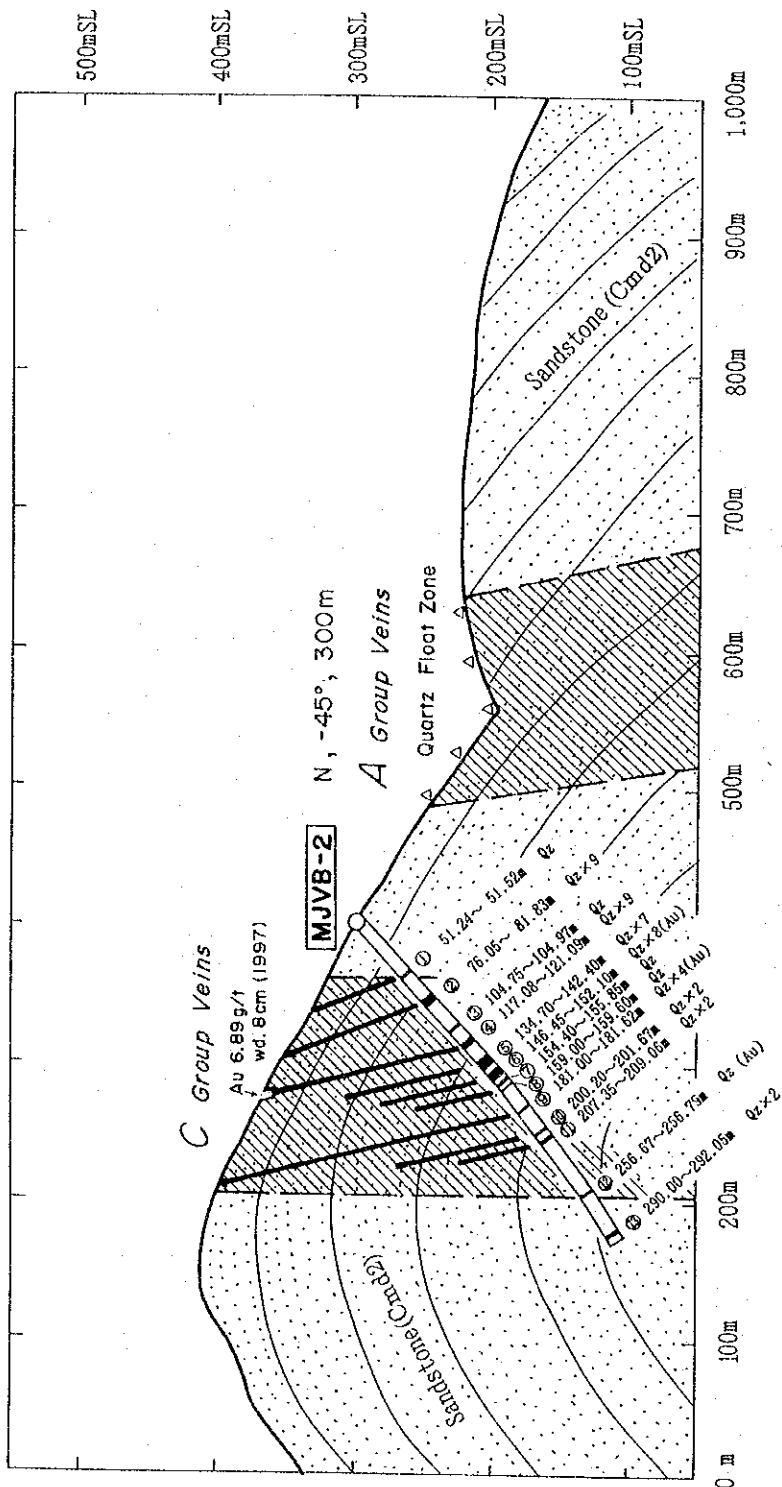
Ser No.	Sample No.	Depth (m)		Sample Width (cm)	Au (g/t)	Ag (g/t)	Cu (%)	Pb (%)	Zn (%)	Fe (%)	Remarks
		From	To								
	MJVB-5										
53	501	26.75	27.10	35	0.019	<0.5	0.002	<0.001	<0.001	1.01	L-gray Qz vein, Limo diss.
54	502	55.58	55.68	10	0.013	<0.5	0.002	0.001	0.007	4.05	White/L-gray Qz veinlets, Limo diss.
55	503	56.62	56.74	12	0.019	<0.5	0.003	0.001	0.005	7.01	White/L-gray Qz veinlets, Limo diss.
56	504	65.40	65.73	33	<0.001	<0.5	0.001	0.001	<0.001	1.21	White Qz vein, Limo diss.
57	506	101.10	101.25	15	0.059	<0.5	0.014	<0.001	0.002	3.21	L-gray Qz vein, Py diss.
58	507	101.95	102.15	20	0.026	0.6	0.001	0.001	0.001	1.41	L-gray Qz vein, Py diss.
59	508	106.00	106.15	15	0.049	<0.5	0.003	0.002	0.003	4.56	L-gray Qz veinlet/breccia, Py diss.
60	509	110.43	110.75	32	0.010	<0.5	0.002	0.002	0.002	3.85	L-gray Qz veinlet/network, Py diss.
61	510	120.10	120.25	15	0.020	<0.5	0.002	0.004	0.003	7.01	L-gray Qz veinlet/network, Py diss.
62	511	142.12	142.58	46	0.041	<0.5	0.004	0.002	0.004	3.15	White/L-gray Qz veins/veinlets, Py diss.
63	512	143.45	143.74	29	0.023	1.1	0.008	0.016	0.007	4.90	White/L-gray Qz veins/veinlets, Py diss.
64	513	144.10	144.50	40	0.037	0.8	0.006	0.003	0.007	4.08	Silicified zone, Blk clayey, Py diss.
65	514	145.00	145.20	20	0.015	<0.5	0.003	0.002	0.003	3.66	Silicified zone, Blk clayey, Py diss.
66	516	170.50	170.80	30	0.091	0.6	0.002	0.002	0.002	5.80	L-gray Qz network, Py diss.
67	523	194.67	194.93	26	0.013	1.1	0.005	0.005	0.007	5.54	L-gray Qz network, Py diss.
68	517	194.97	195.12	15	0.024	<0.5	0.006	0.005	0.010	4.36	L-gray Qz network, Py diss.
69	518	203.70	203.95	25	0.016	0.5	0.005	0.003	0.007	4.62	White/L-gray Qz veinlet/network, Py diss.
70	519	204.18	204.40	22	0.011	<0.5	0.005	0.004	0.008	4.73	White/L-gray Qz veinlet/network, Py diss.
71	520	204.70	205.00	30	0.013	0.5	0.004	0.005	0.008	4.36	White/L-gray Qz veinlet/network, Py diss.
72	521	263.25	263.61	36	0.020	<0.5	0.001	<0.001	0.004	3.49	L-gray Qz veinlets/networks with Chl and Cln, Py diss.
	MJVB-6										
73	618	2.13	2.50	37	0.023	1.1	0.002	0.008	0.003	3.60	Silicified zone with broken Qz.
74	601	2.80	3.10	30	0.034	1.3	0.004	0.016	0.006	6.47	L-gray Qz vein
75	602	4.00	4.50	50	0.011	0.7	0.002	0.021	0.002	1.80	L-gray Qz vein
76	603Y	4.60	4.75	15	0.012	1.4	0.003	0.012	0.009	4.93	L-gray Qz vein/silicified zone, Limo-Py diss.
77	604	6.60	6.80	20	0.010	1.0	0.003	0.006	0.002	3.43	L-gray Qz vein, Limo diss.
78	605Y	20.50	20.70	20	0.010	0.6	0.002	0.003	0.001	2.79	Silicified/shaded zone with Qz veinlets.
79	606	28.00	29.00	100	0.019	1.2	0.007	0.011	0.001	2.22	Clayey zone with Qz veinlets.
80	607	29.00	30.00	100	0.015	0.7	0.002	0.016	0.001	2.08	Clayey zone with Qz veinlets.
81	608	30.00	31.00	100	0.012	0.7	0.002	0.013	0.001	1.66	Clayey zone with Qz veinlets.
82	609	31.00	32.00	100	0.020	0.8	0.003	0.012	0.001	1.60	Clayey zone with Qz veinlets.
83	610	32.00	33.00	100	0.028	<0.5	0.003	0.007	0.001	2.53	Clayey zone with Qz veinlets.
84	611	33.00	34.00	100	0.044	1.0	0.003	0.011	0.001	1.41	Clayey zone with Qz veinlets.
85	612	34.00	35.00	100	0.039	0.7	0.011	0.015	0.001	2.67	Clayey zone with Qz veinlets.
86	613	35.00	36.35	135	0.025	1.0	0.004	0.007	0.001	1.91	Clayey zone with Qz veinlets.
87	614	36.35	36.55	20	0.014	1.1	0.005	0.009	0.001	3.60	L-gray Qz vein.
88	615Y	36.55	37.50	95	0.015	0.5	0.003	0.006	0.002	3.15	Clayey zone.
89	616	37.50	38.10	60	0.040	0.9	0.005	0.009	0.004	3.32	Clayey zone with Qz veinlets.
90	617	54.35	55.25	90	0.081	0.8	0.004	0.003	0.005	4.59	L-gray Qz vein.
91	619Y	68.05	68.15	10	0.107	1.3	0.001	0.001	<0.001	0.79	L-gray Qz vein.
92	620Y	90.80	90.95	15	0.046	0.5	0.006	0.005	0.012	10.39	L-gray Qz veinlets.
93	621	96.40	96.55	15	0.012	0.9	0.003	0.003	0.005	4.17	L-gray Qz vein, Py diss.
94	622	108.15	108.40	25	0.031	0.7	0.005	0.006	0.008	13.43	L-gray Qz veinlet/breccia, Limo diss.
95	624	168.63	168.80	17	0.015	<0.5	0.003	0.003	0.006	3.94	White Qz veinlets, Py diss.
96	625	173.05	173.40	35	0.018	<0.5	0.003	0.004	0.005	4.45	Qz veinlet/stringer zone, Py diss.
97	626	186.95	187.70	75	0.013	<0.5	0.002	0.003	0.005	4.19	White Qz veins/veinlets, Py, Chl & Cln diss.
98	627	188.20	188.73	53	0.023	0.5	0.005	0.003	0.006	4.05	White Qz veins/veinlets, Py diss.
99	628	190.10	190.30	20	0.205	<0.5	0.002	0.003	0.004	3.26	White Qz veins/veinlets, Py diss.
100	629	258.75	259.20	45	0.011	<0.5	0.001	0.001	0.003	2.81	Silicified zone, Py diss.
101	630	279.72	280.30	58	0.012	0.7	0.003	0.005	0.009	5.63	L-gray Qz veinlets/network, Chl (s), Py diss.



Ser	Sample No.	Depth (m)	Sample Width (cm)	Au (g/t)	Ag (g/t)	Cu (%)	Pb (%)	Zn (%)	Fe (%)
13	114A	108.58 - 109.00	42	<0.001	<0.5	0.002	0.004	0.004	3.58
14	115A	110.25 - 110.65	60	<0.001	<0.5	0.001	0.001	0.002	2.15
15	116A	128.55 - 129.90	75	0.011	<0.5	0.008	0.001	0.005	2.91
16	117A	129.30 - 130.37	107	0.001	<0.5	0.001	0.005	0.005	3.24
17	118A	136.50 - 137.00	50	0.002	<0.5	0.013	0.003	0.008	3.60
18	119A	137.00 - 137.50	50	0.003	<0.5	0.002	0.009	0.003	2.15
19	121A	154.65 - 155.21	56	0.008	<0.5	0.001	<0.001	<0.001	0.99
20	122A	155.28 - 155.63	35	0.004	<0.5	0.001	<0.001	<0.001	0.99
21	235A	170.67 - 172.72	205	0.010	<0.5	0.031	0.031	0.051	3.30
22	125A	226.00 - 221.95	135	0.011	<0.5	0.003	0.002	0.006	2.87
23	126A	286.75 - 280.88	13	0.016	<0.5	0.004	0.003	0.006	2.93

Ser	Sample No.	Depth (m)	Sample Width (cm)	Au (g/t)	Ag (g/t)	Cu (%)	Pb (%)	Zn (%)	Fe (%)
1	101A	10.60 - 10.70	10	0.008	<0.5	0.001	<0.001	<0.001	0.30
2	102A	17.00 - 17.90	90	0.004	<0.5	0.001	<0.001	0.001	2.06
3	103A	28.00 - 28.65	65	0.004	<0.5	0.001	0.001	0.007	4.51
4	104A	59.10 - 69.55	48	0.005	<0.5	0.001	<0.001	0.001	3.15
5	124A	96.00 - 97.00	100	0.005	<0.5	0.006	0.004	0.004	3.92
6	105A	97.10 - 97.85	75	0.010	<0.5	0.001	0.001	0.004	3.10
7	106A	98.30 - 98.94	64	0.008	<0.5	0.002	0.001	0.004	2.80
8	107A	99.00 - 99.90	90	0.003	<0.5	0.004	0.003	0.004	2.90
9	109A	104.88 - 105.35	47	<0.001	<0.5	0.001	0.002	0.004	3.10
10	110A	105.55 - 105.85	30	<0.001	<0.5	0.002	0.003	0.004	2.95
11	112A	106.40 - 105.80	40	0.002	<0.5	0.001	0.002	0.004	2.85
12	113A	107.62 - 108.40	78	0.004	<0.5	0.001	0.002	0.003	2.90

Fig. 2-2-8 Geologic Section along the Drill Hole (MJVB-1)



Sample No.	Depth (m)		Sample width (cm)	Au (g/t)	Ag (g/t)	Cu (%)	Pb (%)	Zn (%)	Fe (%)
	From	To							
1	51.24	51.52	28	56.640	9.0	0.009	0.113	0.016	1.88
2	76.88	77.43	55	0.132	<0.5	0.002	0.001	0.001	2.41
3	81.13	81.33	20	0.440	<0.5	0.015	0.000	0.001	2.78
4	104.75	104.97	22	0.070	<0.5	0.002	0.001	0.001	2.06
5	118.02	118.62	60	0.140	<0.5	0.001	0.001	0.001	1.32
6	119.13	119.42	29	0.110	<0.5	0.001	0.001	0.001	1.34
7	120.81	121.05	24	0.450	<0.5	<0.001	<0.001	0.001	3.26
8	137.38	137.57	49	0.138	<0.5	<0.001	<0.001	0.001	1.47
9	138.00	138.40	40	1.880	2.0	0.012	0.008	0.001	3.10
10	141.30	141.48	16	0.112	<0.5	0.003	0.001	0.003	3.61
11	143.30	143.30	40	0.185	<0.5	0.001	0.001	0.002	2.83
12	146.45	146.66	21	0.036	<0.5	0.001	0.006	0.034	2.64
13	148.20	149.15	95	0.007	<0.5	0.003	0.001	0.001	1.63
14	149.15	150.00	85	0.011	<0.5	0.001	<0.001	0.001	1.81
15	150.00	151.05	105	0.055	<0.5	0.001	<0.001	0.001	2.38

Sample No.	Sample No.	Depth (m)		Sample width (cm)	Au (g/t)	Ag (g/t)	Cu (%)	Pb (%)	Zn (%)	Fe (%)
		From	To							
16	215A	151.05	152.10	105	0.040	<0.5	0.001	<0.001	0.001	1.84
17	217A	154.40	155.85	145	0.059	<0.5	0.001	0.002	0.011	2.13
18	218A	159.00	159.60	60	0.067	1.0	0.001	0.005	0.007	3.39
19	219A	181.00	181.11	11	1.020	<0.5	0.008	<0.005	0.013	4.43
20	242A	181.11	181.22	11	0.120	<0.5	0.010	0.006	0.021	2.65
21	220A	181.22	181.32	10	0.0815	<0.5	0.001	0.001	0.002	2.54
22	244A	181.32	181.57	25	0.050	<0.5	0.005	<0.005	0.014	2.42
23	245A	181.57	181.80	23	0.050	<0.5	0.005	<0.005	0.010	3.78
24	222A	200.30	200.30	10	0.136	<0.5	<0.001	<0.001	0.001	5.57
25	223A	201.36	201.67	32	0.154	<0.5	0.001	<0.001	0.001	4.00
26	224A	208.20	208.20	85	0.055	<0.5	0.118	0.001	0.001	1.86
27	225A	208.40	209.05	66	0.072	<0.5	0.001	<0.001	0.001	2.69
28	226A	256.67	256.78	12	1.400	<0.5	0.016	0.160	0.031	3.14
29	227A	290.00	290.72	72	0.090	<0.5	0.012	0.006	0.029	2.90
30	228A	291.45	292.05	60	0.010	<0.5	0.010	0.008	0.032	2.28

Fig. 2-2-9 Geologic Section along the Drill Hole (MJVB-2)

2-6-4 Mineralization

Two holes totaling 600.00 m were drilled in the central to the western part of the Da Mai-Khe Dui prospect in the second phase. As was described in the previous section, a significant amount of gold-bearing quartz veins were intersected in these drill holes. They were classified into more than ten groups of veins in each hole on the basis of the vein nature (similarity of ore, gangue and alteration mineralogy, morphological and spatial closeness).

MJVB-1: This drill hole is located at the upper reaches of Da Mai creek in the Da Mai-Khe Dui prospect. The main purpose of this hole was to investigate the lower extension of the Group A veins of the Da Mai-Khe Dui prospect. Thirteen major groups of veins were caught in this hole in total. The outline of the mineralization and hydrothermal alteration is summarized as follows.

- (1) 7.13 – 11.47 m: Quartz vein/veinlet zone, consisting of more than 10 white/light gray quartz veins/veinlets (0.5 to 10 cm wide each) with small amount of limonite.
- (2) 15.58 – 17.90 m: Quartz veinlet/network zone, consisting of 3 white milky quartz veinlets (2 to 90 cm each). No sulfide mineral was observed.
- (3) 25.95 – 28.50 m: Quartz vein/veinlet zone, consisting of white milky quartz veins/veinlets (1 to 55 cm wide each). Partly chloritized.
- (4) 35.90 – 37.00 m: Two white quartz veins, 33 cm and 45 cm. No sulfide mineral was observed.
- (5) 67.39 – 71.27 m: Quartz vein/veinlet zone, consisting of 6 white/gray quartz veins/veinlets (6 to 67 cm wide each) with weak pyrite dissemination. The host rock was strongly silicified. Two categories of quartz were distinguished; earlier deposited gray quartz and later white quartz. The former contains a small amount of sulfide minerals such as pyrite, arsenopyrite and chalcopyrite.
- (6) 91.50 – 99.90 m: Quartz vein/breccia zone, consisting of 13 white/gray quartz veinlets/breccias (2 to 90 cm wide each). Pyrite, arsenopyrite and chalcopyrite were disseminated partly. Quartz is cut by calcite veinlets. Chloritization and sericitization were observed in some part. Several gold grains were found in slime of drilling, and a very small gold grain was observed in drill cores by naked eye.
- (7) 104.88 – 112.60 m: Quartz vein/breccia zone, consisting of 7 white/gray quartz veins/breccias (10 to 60 cm wide each). Pyrite was disseminated partly. Pyrite, arsenopyrite, pyrrhotite, chalcopyrite, sphalerite, galena and anglesite were found under the microscope. Chloritization was observed in some part. Several gold grains were found in slime of drilling, and a couple of tiny free gold were observed in drill cores by naked eye.
- (8) 128.55 – 130.37 m: Quartz vein/veinlet zone, consisting of 6 white quartz veins/veinlets (5 to 30 cm wide each). Pyrite was slightly disseminated. Chloritization was observed in some part.
- (9) 136.50 – 137.50 m: Quartz vein/veinlet zone, consisting of 2 white quartz veins (31 and 53 cm wide each). Pyrite, chalcopyrite and sphalerite were disseminated partly. Chloritization was observed in some part. A couple of free gold was observed in drill cores by naked eye.

(10) 154.65 – 156.43 m: Quartz vein/veinlet zone, consisting of 4 gray quartz veins/veinlets (4 to 35 cm wide each) with small amount of pyrite. Chloritization was observed in some part. A couple of gold grains were observed in drill cores by naked eye.

(11) 170.67 – 172.72 m: White to light gray quartz vein of about 20 cm in true width running nearly parallel to the drill hole. Chloritization was observed partly. Sulfide minerals such as pyrite and arsenopyrite are weakly disseminated.

(12) 219.68 – 221.35 m: Quartz veinlet zone, consisting of 10 gray quartz veinlets (2 to 5 cm wide each). No sulfide mineral was observed.

(13) 280.75 – 280.88 m: Light gray quartz vein of 13 cm wide. Host rock is strongly silicified. A couple of gold grains were detected in slime of drilling.

MJVB-2: This drill hole is located at the upper reaches of West Da Mai creek in the Da Mai-Khe Dui prospect. The main purpose of this hole was to investigate the lower extension of the Group C veins of the Da Mai-Khe Dui prospect. Thirteen major groups of veins were caught in this hole in total. Several significant assay results of Au and Ag were obtained in this drill hole. The outline of the mineralization and hydrothermal alteration is summarized as follows.

(1) 51.24 – 51.52 m: Gray quartz vein/silicified zone (28 cm wide). Quartz is coarse grain and porous (drusy). Limonite and pyrite are disseminated in quartz. Host sandstone is strongly silicified. A couple of gold grains were found from slime of drilling. An assay result of **56.640 g/t Au** and **9.0 g/t Ag** was obtained from this zone. The content of galena is also significant up to **1,130 ppm Pb**.

(2) 76.05 – 81.83 m: Gray quartz vein/veinlet zone, consisting of 9 gray to light gray quartz veins/veinlets (1 to 55 cm wide each). The thickest (76.88 – 77.43 m) among them is light gray quartz vein, which contains a small amount of pyrite and arsenopyrite. Quartz sometimes shows a brecciated texture. Chloritization was observed. Several gold grains (medium to fine or very fine carat) were detected in slime of drilling.

(3) 104.75 – 104.97 m: A gray quartz vein (15 cm wide) occurs. The boundary of footwall is irregular (brecciated).

(4) 117.08 – 121.09 m: Gray quartz vein/network zone, consisting of 9 gray to light gray quartz veins/networks (1 to 57 cm wide each). Three significant quartz networks were caught in this zone: 118.02 – 118.62, 119.13 – 119.42, and 120.81 – 121.09 m. A small amount of pyrite is disseminated. Several gold grains (medium to fine or very fine carat) were found from slime of drilling.

(5) 134.70 – 142.40 m: Gray/white quartz vein/network zone, consisting of more than 8 gray to light gray and white quartz veins/networks (3 to 50 cm wide each). Four significant quartz networks were caught in this zone: 135.00 – 135.40, 137.38 – 137.87, 138.90 – 139.30, and 141.30 – 141.46 m. In these quartz veins/networks, a small amount of sulfide minerals such as pyrite, arsenopyrite, pyrrhotite and chalcopyrite were observed. Both white and gray quartz contains sulfide minerals. Several gold

grains (medium to fine or very fine carat) were returned from slime of drilling. An assay result of **1.880 g/t Au** and **2.0 g/t Ag** was returned from one of quartz networks (49 cm in width, 137.38 – 137.87 m).

(6) 146.45 – 152.10 m: Gray quartz vein/network zone, consisting of more than 8 light gray/gray quartz veins/veinlets and networks (1 to 195 cm wide each). Three significant quartz veins/networks were caught in this zone: 146.45 – 146.66, 148.20 – 150.00, and 150.00 – 152.10 m. In these quartz veins/networks, a small amount of sulfide minerals such as pyrite, arsenopyrite, pyrrhotite and chalcopyrite were observed. There were two kinds of quartz – white and gray/light gray -- were distinguished; the former cut the latter. Chlorite is contained in some part of quartz near the fragments of host rock in quartz. A couple of tiny gold grains were observed in drill cores by naked eye. Several gold grains (medium to fine or very fine carat) were returned from slime of drilling.

(7) 154.40 – 155.85 m: Gray quartz veinlet zone, consisting of several gray to light gray quartz veinlets (0.5 to 1 cm wide each). Silicified and decolorized.

(8) 159.00 – 159.60 m: Gray/white quartz vein (60 cm wide). Pyrite is weakly disseminated. The surrounding host rock (sandstone, 20 to 90 cm) is decolorized by strong silicification.

(9) 181.00 – 181.62 m: Gray quartz veinlet zone, consisting of 5 gray quartz veinlets (1 to 10 cm wide each). Pyrite and chalcopyrite are disseminated. Chlorite is contained in quartz. Several small grains of native gold (up to 0.5 mm long) were observed by naked eye. Gold assays such as **1.020 g/t Au** (11 cm in width, 181.00 – 181.11 m) and **10.815 g/t Au** (10 cm in width, 181.22 – 181.32 m) were obtained.

(10) 200.20 – 201.67 m: Light gray quartz vein zone, consisting of 2 light gray quartz veins (10 and 32 cm). Quartz is brecciated. Pyrite and pyrrhotite are disseminated (spotted). The content of sulfide minerals is significant up to **5.57 % Fe** (200.20 – 200.30 m). Strong silicification and chloritization were observed.

(11) 206.88 – 209.06 m: White/light gray quartz vein zone, consisting of 2 white/light gray quartz veins (66 and 85 cm). Light gray quartz is cut by white quartz vein. Pyrite, arsenopyrite, pyrrhotite and chalcopyrite are disseminated. The dissemination of chalcopyrite was significant up to **1,180 ppm Cu** (207.35 – 208.20 m). Strong silicification, chloritization and sericitization were observed.

(12) 256.67 – 256.79 m: Gray silicified zone, consisting of gray silicified sandstone cut by white quartz veinlet (1 to 2 cm wide). Pyrite, arsenopyrite and galena are disseminated. The dissemination of galena is significant up to **1,600 ppm Pb** (256.67 – 256.79 m). A couple of tiny gold grains were found in this silicified zone near a white quartz veinlet. Gold assay was **1.400 g/t Au** in this zone.

(13) 290.00 – 292.05 m: Gray quartz vein zone, consisting of 2 gray to light gray quartz veins (72 and 60 cm). Quartz is brecciated. Pyrite and chalcopyrite are disseminated. Strong silicification and chloritization were observed.

2-6-5 Fluid Inclusion Studies

(1) Methodology

Quartz chips of the drill cores were collected, and provided for fluid inclusion studies. More than ten quartz chips were sampled from drill cores. All samples were taken from quartz veins. The same methods and measurements as in the detailed geological survey were made for the studies.

(2) Results of Studies

The total number of fluid inclusions which were investigated under the microscope was 103. More than eighty percents of them are liquid-rich two-phase inclusions. Gas-rich two-phase inclusions are less than 20 % of them. This result may indicate that the boiling of fluid has occurred locally during the formation of quartz vein.

Polyphase inclusions were found in 5 samples. Halite was distinguished as a daughter mineral.

Homogenization Temperature

Values of homogenization temperature of each fluid inclusion are distributed from 145°C to 340°C. Most of them fall into a range of 160° ~ 300°C with a peak value of 210°C.

Salinity

Samples for the measurement of freezing temperature were selected from quartz chips of which homogenization temperature was measured. Three measurements on salinity for 2 fluid inclusions from the drill core MJVB-1 were carried out in this study.

Salinity calculated from the freezing temperatures of fluid inclusions ranges from 4.1 to 5.7 wt. % NaCl equivalent. The arithmetic mean of three salinity values is 4.8 wt. % NaCl equiv.

2-7 Drilling (Phase III)

2-7-1 Outline of Drilling

Following the reconnaissance drilling in the second phase, a diamond drilling program comprising four holes totaling 1,200 m was planned in the Da Mai and Ngan Me areas in the third phase. These holes were directed towards the significant geological/geochemical and geophysical anomalous zones. Magnificent gold mineralized zones at the Da Mai-Khe Dui prospect, which were defined by geological/geochemical and IP geophysical surveys were targeted by two holes -- MJVB-3 and 4. Significant gold mineralized zones at the Ba Khe prospect, which were also outlined by geological/geochemical and IP geophysical surveys were tested by another two holes -- MJVB-5 and 6.

The drilling program was composed of inclined holes of 300 m deep each. Target depths were set at 50 to 250 m from the surface. Details of each hole are summarized in the table in the third phase report. The location map of drill holes is shown in Fig. 2-2-7.

Hole No.	Area & Prospect	Location	Latitude (N)	Longitude (E)	Elevation (m)	Azimuth	Inclination (°)	Length (m)
MJVB-3	Da Mai-Khe Dui (Da Mai Area)	Khe Dui Creek	21°40'34"	106°00'58"	320	N	-45	300.00
MJVB-4	Ditto	Khe Dui Creek	21°40'40"	106°00'50"	260	N	-45	300.00
Total	2 holes							600.00

A series of drill logs of 1:200 scale was prepared, and the whole drill cores were photographed in color. A total of 101 samples for ore assay was obtained. Six elements (Au, Ag, Cu, Pb, Zn and Fe) were analyzed for ore assay. Twenty polished sections for ore microscopy and twenty thin sections for petrography were produced from the cores. Twenty-one altered rock and quartz samples were examined for X-ray powder diffraction analysis. Ten quartz samples were provided for fluid inclusion studies. (Amount of samples are both in Da Mai and Ngan Me)

2-7-2 Method, Equipment and Progress

(1) Method and Equipment

Method

For the near-surface weathered zone (2 to 4 m), drilling was normally done by PQ size metal bit (132 mm in diameter) with inserting of PW drive pipes (146 mm in inner diameter). Weakly weathered bedrock and the upper part of bedrock zone (down to 100 to 150 m) were drilled by the conventional drilling method using HQ size diamond bit (91 mm in diameter). The weakly weathered bedrock continued to 20 to 40 m deep. Reaming at 117 mm in diameter was done by using diamond or metal bit, and HW casing pipes (108 mm in inner diameter) were inserted in this zone. For the upper part of bedrock zone, NW casing pipes (89 mm in inner diameter) were inserted down to approximately 100/150 m. From 100/150 m to 300 m (the end of hole), drilling was made with NQ size diamond bit (76 mm in diameter) and NQ-WL core tube. Bentonite clay, polymer (CMC) and NaOH (pH adjustment agent) were usually mixed in the circulating drilling water. When the water was lost at a depth where fractures were developed, a natural fibrous material (commercial name is GPC made in China) was injected to recover the trouble. When the fracture was significantly wide, half-solid bentonite clay was inserted.

Equipment

A set of Russian ZIF-650M drilling machine, a set of Long-Year L-38 drilling machine and two sets of Russian NB-3 drilling pumps were brought into operation in this exploration. One drill rig was a Vietnamese domestic-made angled tripod-type for the ZIF-650M machine. Another one was a ladder-type rig equipped with the L-38 machine. Specifications of drilling machine and equipment are shown in Table 2-2-4. Diamond bits and expendable items used during the drilling are listed in tables in the third phase report.

Working System

Drilling operation was carried out by three shifts per day (8 hours per shift), while the appurtenant works, such as rig construction, mobilization and demobilization, were done by one shift per day (8 to 10 hours). A shift crew consisted of one drilling engineer and three to four workers normally. Additional twenty workers (round figures) were involved in case of the appurtenant work. A series of base camps for drilling operation were built at the foot of creeks.

Transportation

The drilling machine and equipment were transported to the survey area by a convoy of 7-ton trucks and 12-ton trucks. A couple of 4-WD trucks (2 to 5 tons in capacity) and a bulldozer were chartered for the transportation of drilling machine and equipment from the main road to the drilling sites through a series of roads which was constructed for this drilling purpose for about 4 km in total. The transportation from the Da Mai area to the Ngan Me area was carried out by a series of trucks and bulldozer.

Supply for the camp was made a couple of times in a week. Fuel and foods were bought at Thai Nguyen, and were transported by chartered cars.

Drilling Water

Water for drilling was pumped up from the middle reaches of creeks to the drilling sites via pipelines whose length was about 2 km for each area. The difference of altitudes between pumping station to the drilling sites was nearly 200 m. Mud water was also prepared in that pumping station, and sent through the pipeline to the drilling sites.

Withdrawal

After the completion of drilling program, the machine and equipment were withdrawn by trucks through the route to Hanoi via Thai Nguyen. The drill holes were capped, and drilling sites were cleaned and reclaimed. The drilling cores, of which some part was taken for assay samples, were kept in the storage house in the office of the NE Geological Division of DGMV, Thai Nguyen.

(2) Progress of Drilling

The progress of each drill hole is described below. The summary of working time, records of drilling operation, records of drilling performance, and charts of drilling progress are shown in tables and figures in the third phase report.

MJVB-3: For the near-surface weathered zone (3.50 m), drilling was done by PQ size metal bit (132 mm in diameter) with inserting of drive pipes (146 mm in inner diameter). Weakly weathered bedrock and the upper part of bedrock zone (down to 100 m) were drilled by the conventional drilling method using HQ size diamond bit (91 mm in diameter) for the maximum core recovery. The weakly weathered bedrock continued to 20 m deep. Reaming at 117 mm in diameter was done by using

diamond and metal bits, and HW casing pipes (108 mm in inner diameter) were inserted in this zone (20.00 m). For the upper part of bedrock zone, NW casing pipes (89 mm in inner diameter) were inserted down to 102.60 m. From 102.60 m to 300 m (the end of hole), drilling was made with NQ size diamond bit (76 mm in diameter) and NQ-WL core tube.

Bentonite clay, polymer (CMC) and NaOH (pH adjustment agent) were usually mixed in the circulating drilling water. The circulating water was lost in the hole at 32.30 and 117.45 m where fractures were developed.

Drill hole survey was made using a Toropali survey instrument. The results of survey for inclination were: -45° at 0 m, -48° at 100 m, -51° at 200 m, and -56° at 300 m. The recovery of cores was 99 % in total because of careful drilling operation.

MJVB-4: For the near-surface weathered zone (3.00 m), drilling was done by PQ size metal bit (132 mm in diameter) with inserting of drive pipes (146 mm in inner diameter). Weakly weathered bedrock and the upper part of bedrock zone (down to 150 m deep) were drilled by the conventional drilling method using HQ size diamond bit (91 mm in diameter) for the maximum core recovery. The weakly weathered bedrock continued to 14 m deep. Reaming at 117 mm in diameter was done by using diamond and metal bits, and HW casing pipes (108 mm in inner diameter) were inserted in this zone (14.35 m). For the upper part of bedrock zone, NW casing pipes (89 mm in inner diameter) were inserted down to 153.60 m.

From 153.60 m to 300 m (the end of hole), drilling was made with NQ size diamond bit (76 mm in diameter) and NQ-WL core tube.

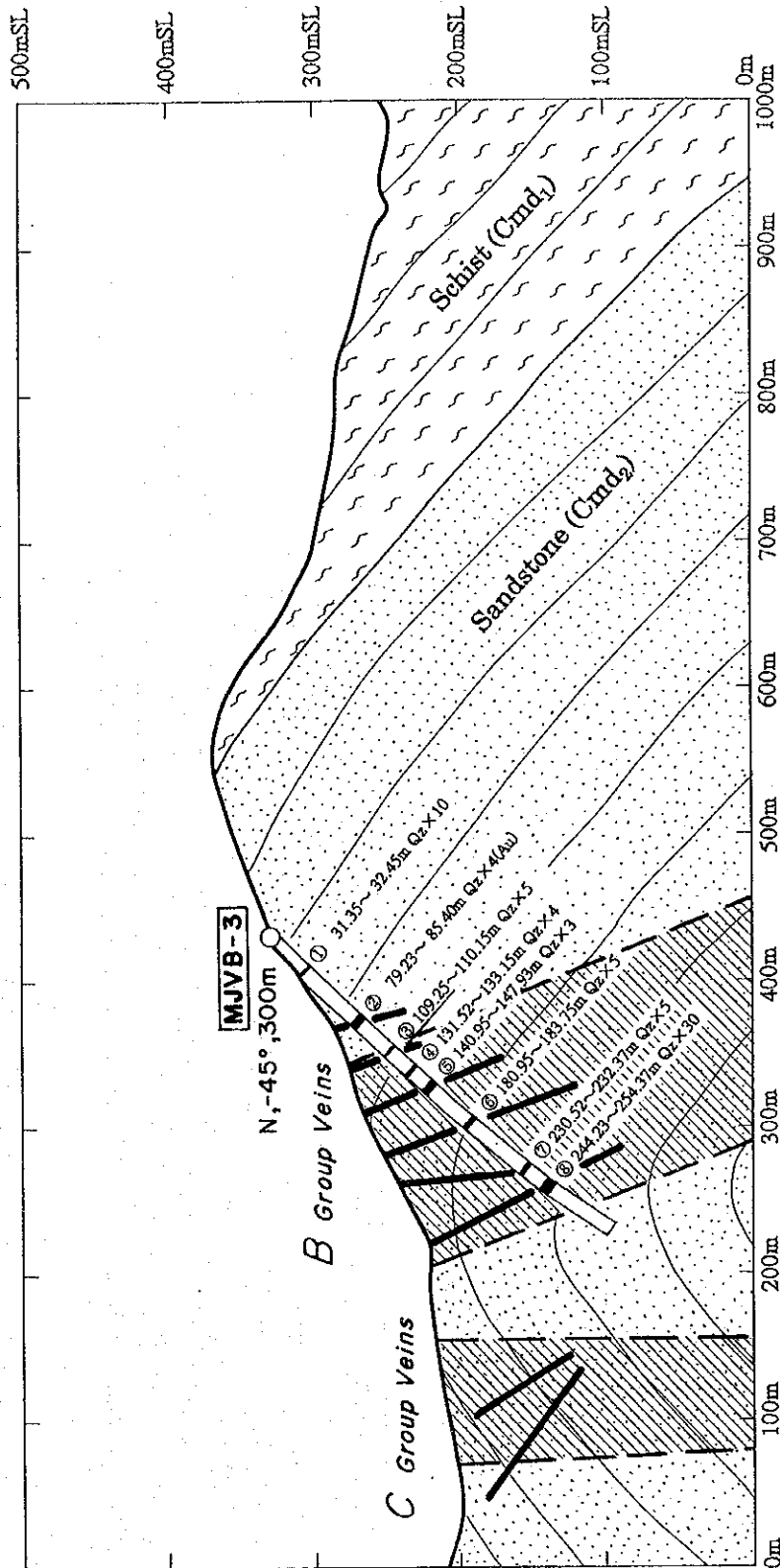
Bentonite clay, polymer (CMC) and NaOH were usually mixed in the circulating drilling water. No water loss has been recorded during drilling.

Drill hole survey was made using a Toropali survey instrument. The results of survey for inclination were: -45° at 0 m, -50° at 100 m, -55° at 200 m, and -51° at 300 m. The overall core recovery was 99.9 % in this hole.

2-7-3 Geologic Description of Drill Holes

The geology of the area where drilling exploration was carried out in the third phase is composed of schist and sandstone of the Mo Dong Formation (C_{md2}).

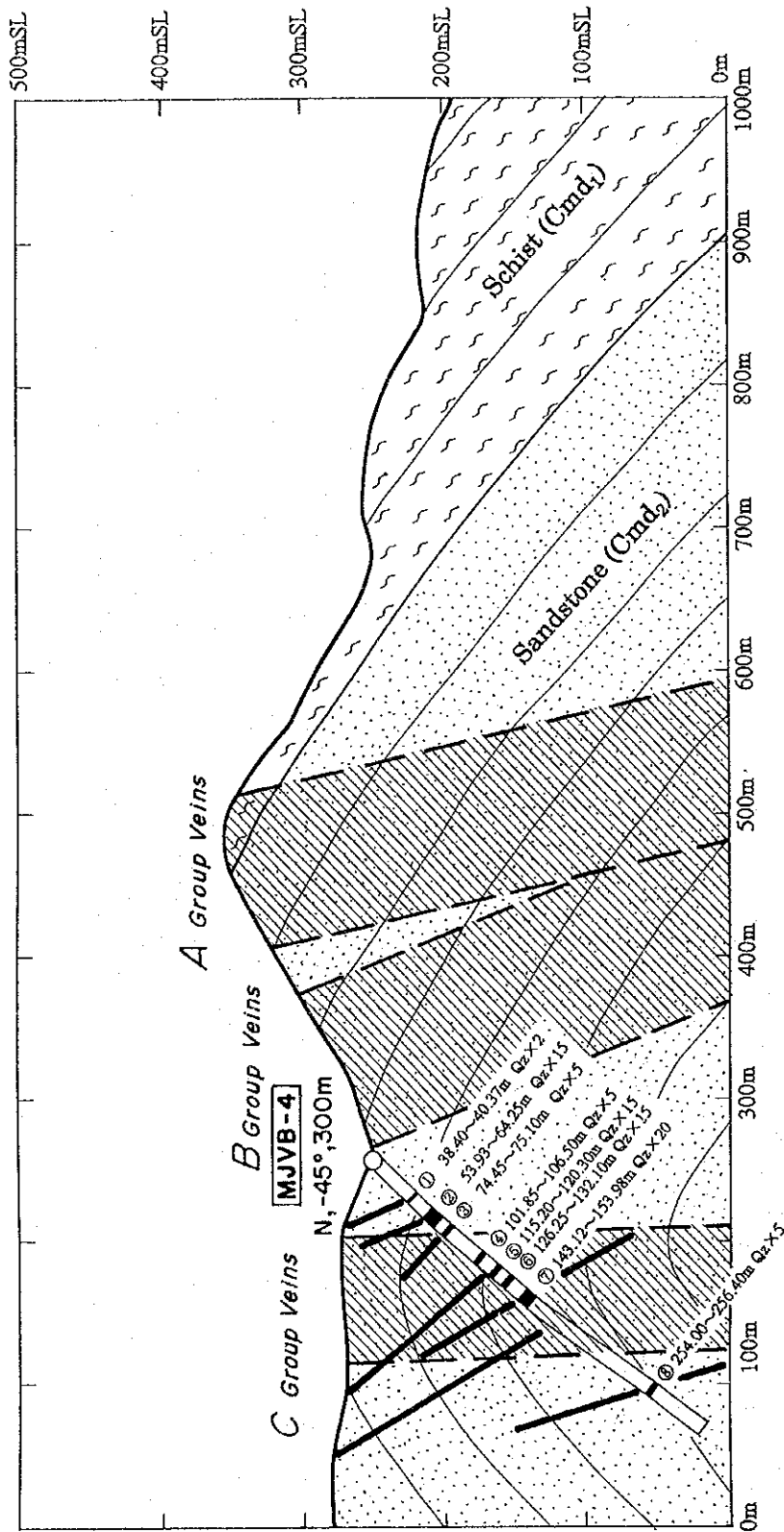
Weathered schist and sandstone occur below the surface soil (a few to 30 cm thick), and extends to nearly 2 to 4 m deep along the drill hole (every hole has drilled at an angle of -45 degrees). Bedrock appears below 10 to 20 m in depth. The results of laboratory works and assaying of drill cores are briefly listed in Tables 2-1-1 to 2-1-3 and 2-2-5. Drill hole sections are shown in Figs. 2-2-10 and 2-2-11.



Ser. No.	Sample No.	Depth (m)		Sample Width (cm)	Au (g/t)	Ag (g/t)	Cu (%)	Pb (%)	Zn (%)	Fe (%)
		From	To							
14	314	175.32	175.55	23	0.150	<0.5	0.002	0.009	0.003	1.80
15	315	180.95	181.08	13	0.020	<0.5	0.005	0.001	0.005	4.56
16	328Y	183.00	183.15	15	0.014	<0.5	0.001	0.001	0.005	4.56
17	316	183.50	183.75	25	0.020	<0.5	0.001	0.001	0.002	1.75
18	318	230.77	231.14	37	0.570	<0.5	0.001	0.001	0.001	3.15
19	329Y	232.20	232.37	17	<0.001	<0.5	0.004	0.003	0.002	3.55
20	319	244.23	244.42	19	0.160	<0.5	0.003	0.001	0.001	2.48
21	320	244.98	245.68	72	0.100	<0.5	0.002	0.002	0.001	4.90
22	330Y	247.10	247.20	10	0.014	<0.5	0.001	<0.001	0.001	1.80
23	321	247.55	248.34	79	0.050	<0.5	0.002	0.001	0.003	4.73
24	331Y	250.10	250.40	30	0.025	<0.5	0.003	0.001	0.005	6.19
25	322	263.40	263.95	55	0.020	1.0	0.003	0.001	0.005	4.34
26	323	273.00	273.15	15	0.020	<0.5	0.001	0.002	0.001	1.92

Ser. No.	Sample No.	Depth (m)		Sample Width (cm)	Au (g/t)	Ag (g/t)	Cu (%)	Pb (%)	Zn (%)	Fe (%)
		From	To							
1	301	31.35	31.90	55	0.020	0.6	0.003	<0.001	0.003	6.48
2	302	32.22	32.45	23	0.010	<0.5	0.028	0.001	0.004	5.57
3	325Y	76.23	79.30	7	0.015	0.7	0.002	<0.001	0.007	4.98
4	305	78.37	79.50	13	0.020	<0.5	0.003	<0.001	0.005	3.71
5	306	79.85	80.20	35	75.600	3.0	0.005	0.001	0.005	3.77
6	307	84.97	85.40	43	0.310	<0.5	0.002	0.002	0.001	1.52
7	308	103.90	104.08	18	0.030	<0.5	0.001	0.003	0.002	2.14
8	310	105.25	110.15	90	0.020	<0.5	0.008	0.002	0.004	3.99
9	311	131.70	132.03	33	0.070	<0.5	0.001	0.001	0.004	3.66
10	326Y	132.95	133.15	20	0.012	<0.5	0.001	0.001	0.005	5.06
11	312	141.74	141.92	16	0.020	<0.5	0.001	0.018	0.003	2.59
12	313	147.60	147.95	33	1.770	<0.5	0.006	0.003	0.010	6.48
13	327Y	154.05	154.12	7	0.053	<0.5	0.003	0.008	0.005	4.50

Fig. 2-2-10 Geologic Section along the Drill Hole (MJVB-3)



Ser No.	Sample No.	Depth (m)		Sample Wt (g)	Au (g/t)	Ag (g/t)	Cu (%)	Pb (%)	Zn (%)	Fe (%)
		From	To							
14	416	145.40	145.50	10	0.010	<0.5	0.004	0.001	0.008	4.22
15	417	145.53	145.58	35	0.020	<0.5	0.004	0.002	0.004	3.10
16	418	146.00	146.55	65	0.010	<0.5	0.003	0.001	0.003	2.59
17	419	147.00	147.55	55	0.010	<0.5	0.002	0.001	0.003	1.07
18	420	148.10	149.05	95	0.010	<0.5	0.003	0.002	0.007	3.10
19	421	153.04	153.53	49	0.200	<0.5	0.004	0.001	0.007	3.88
20	422	153.65	153.75	10	0.020	<0.5	0.004	0.001	0.007	3.82
21	423	153.90	153.95	8	0.020	<0.5	0.001	0.003	0.006	3.27
22	424	157.70	158.03	33	0.010	<0.5	0.003	0.001	0.004	2.14
23	425	161.25	161.40	17	0.020	<0.5	0.003	0.008	0.008	2.64
24	426	192.80	193.20	40	0.010	<0.5	0.001	0.002	0.004	1.24
25	428	254.00	254.45	45	0.010	<0.5	0.002	0.001	0.002	2.56
26	429	256.29	256.40	11	0.120	<0.5	0.001	0.015	0.001	0.96

Ser No.	Sample No.	Depth (m)		Sample Wt (g)	Au (g/t)	Ag (g/t)	Cu (%)	Pb (%)	Zn (%)	Fe (%)
		From	To							
1	401	38.40	38.80	40	0.020	0.5	0.001	0.005	0.004	2.93
2	402	40.05	40.37	32	0.010	<0.5	0.002	0.002	0.002	2.59
3	403	53.93	54.47	54	0.020	<0.5	0.003	0.003	0.007	3.67
4	404	60.15	60.60	45	12.400	0.6	0.005	<0.001	0.007	4.22
5	405	74.45	75.10	65	0.120	<0.5	0.004	0.002	0.008	4.28
6	407	102.45	102.94	49	0.110	<0.5	0.001	0.002	0.012	1.86
7	409	115.48	115.64	16	0.050	<0.5	0.002	<0.001	0.004	2.31
8	410	116.67	117.95	128	0.050	<0.5	0.005	0.001	0.005	4.22
9	411	118.55	118.95	40	0.010	<0.5	0.003	0.003	0.002	1.80
10	430Y	119.08	119.60	52	0.012	<0.5	0.007	0.004	0.011	5.01
11	412	126.25	127.30	105	0.020	<0.5	0.003	<0.001	0.004	2.36
12	413	131.65	132.10	45	0.060	<0.5	0.005	0.002	0.005	5.06
13	415	143.40	143.75	35	0.020	<0.5	0.002	<0.001	0.005	2.59

Fig. 2-2-11 Geologic Section along the Drill Hole (MJVB-4)

MJVB-3: The geology around the drill hole MJVB-3 is composed of sandstone and schist of the Mo Dong Formation. It is located at the upper reaches of Khe Dui creek. The altitude of the drill hole is about 320 m above sea level. The purpose of this hole was to investigate the lower extension of gold mineralization in the eastern part of the Da Mai-Khe Dui prospect. It mainly targeted at the Group B veins in the Da Mai-Khe Dui prospect. The geology of the drill hole is composed of an alternating bed of sandstone and schist. The upper part is mainly composed of gray sandstone. Whereas, the lower part is composed of an alternation of black schist and gray sandstone. The details of geology of the drill hole were described in the third phase report.

MJVB-4: The geology around the drill hole MJVB-4 is composed of schist and sandstone of the Mo Dong Formation. It is located at the upper reaches of Khe Dui creek. The altitude of the drill hole is about 260 m above sea level. The purpose of this hole was to investigate the lower extension of gold mineralization in the eastern part of the Da Mai-Khe Dui prospect. It mainly targeted at the Group C veins in the Da Mai-Khe Dui prospect. The geology of the drill hole is composed of an alternating bed of sandstone and schist. The upper part and lower part are composed of an alternation of black schist and gray sandstone. Whereas, the middle part is mainly composed of black schist. The details of geology of the drill hole were described in the third phase report.

2-7-4 Mineralization

Two holes totaling 600.00 m were drilled in the central to the western part of the Da Mai-Khe Dui prospect in the third phase. As was described in the previous section, a significant amount of gold-bearing quartz veins were intersected in these drill holes. They were classified into several groups of veins in each hole on the basis of the vein nature (similarity of ore, gangue and alteration mineralogy, morphological and spatial closeness).

MJVB-3: This drill hole is located at the upper reaches of Khe Dui creek in the Da Mai-Khe Dui prospect. The main purpose of this hole was to investigate the lower extension of the Group B veins at the eastern side of the Da Mai-Khe Dui prospect. A total of eight major groups of veins were caught in this hole. Several significant assay results of Au, though not wide, were obtained in this drill hole. The outline of the mineralization and hydrothermal alteration is summarized as follows.

(1) 31.35 – 32.45 m: Quartz veinlet zone, consisting of several white/light gray quartz veinlets (0.5 to 3 cm wide each) with small amount of pyrite and limonite. Clayey. Several gold grains (fine to medium carat) were found in slime of drilling.

(2) 79.23 – 85.40 m: Quartz vein/veinlet zone, consisting of 4 white to light gray quartz veins/veinlets (7 to 43 cm each). Calcite is associated with quartz in some part. Pyrite and limonite are disseminated moderately (strongly in some part). A tiny grain of native gold was found at about 80 m in drill cores. Several gold grains (fine carat) were detected in slime of drilling. A significant assay result of **75.600 g/t Au and 3.0 g/t Ag at 35 cm in width** (79.85 – 80.20 m) was obtained in this zone.

(3) 109.25 – 110.15 m: Quartz veinlet/network zone, consisting of white to light gray quartz veinlets and network (a few cm wide). Partly chloritized. Pyrite is disseminated weakly.

(4) 131.52 – 133.15 m: Four white/light gray quartz veins/veinlets, a few cm to 33 cm. Two categories of quartz were distinguished; earlier deposited gray quartz and later white quartz. Chlorite and a clay mineral (yellowish color) are associated with quartz. Pyrite and arsenopyrite are disseminated weakly. A small amount of chalcopyrite, sphalerite, galena and pyrrhotite were observed under the microscope. Several gold grains (fine carat) were detected in slime of drilling.

(5) 140.95 – 147.93 m: Quartz vein/network zone, consisting of white to light gray quartz veins and network (12 to 33 cm wide each). Chlorite and calcite are associated with quartz. Pyrite is disseminated moderately to strongly. An assay result of **1.770 g/t Au at 33 cm in width** (147.60 - 147.93 m) was returned from one of the quartz network.

(6) 180.95 – 183.75 m: Quartz vein/veinlet zone, consisting of 5 white/light gray quartz veins/veinlets (1 to 25 cm wide each) with pyrite-arsenopyrite dissemination. Chlorite is partly associated with quartz.

(7) 230.52 – 232.37 m: Quartz vein/breccia zone, consisting of 5 white/light gray quartz-calcite veinlets/breccias (a few cm to 37 cm wide each). Pyrite and arsenopyrite are disseminated partly. An assay result of **0.570 g/t Au at 37 cm in width** (230.77 – 231.14 m) was returned.

(8) 244.23 – 254.37 m: Quartz veinlet/network zone, consisting of more than 30 white/light gray quartz veinlets/breccias (a few cm up to 47 cm wide each). Pyrite and arsenopyrite are disseminated partly (weakly in general). A small amount of chalcopyrite and sphalerite were observed under the microscope. Silicification in almost all the zone. Chloritization was observed in some part.

MJB-4: This drill hole is located at the upper reaches of Khe Dui creek in the Da Mai-Khe Dui prospect. The main purpose of this hole was to investigate the lower extension of the Group C veins at the eastern side of the Da Mai-Khe Dui prospect. Eight major groups of veins were caught in this hole in total. A significant assay result of Au, though also narrow, was obtained at the shallow part of this drill hole. The outline of the mineralization and hydrothermal alteration is summarized as follows.

(1) 38.40 – 40.37 m: Light gray quartz veins (40 and 27 cm wide each) with some calcite and chlorite. Pyrite is disseminated weakly in quartz. A small amount of arsenopyrite, chalcopyrite, sphalerite, galena and pyrrhotite were observed under the microscope.

(2) 53.93 – 64.25 m: White quartz-calcite veinlet zone, consisting of 15 white quartz veinlets (2 to 7 cm wide each). Quartz is coarse grain, sometimes appears drusy. Pyrite, arsenopyrite and chalcopyrite are disseminated in quartz. More than ten gold grains (coarse to medium carat) were recovered in slime of drilling by panning. An assay result of **12.400 g/t Au at 45 cm in width** (60.15 – 60.60 m) was returned.

(3) 74.45 – 75.10 m: White quartz-calcite veinlets (a few to 8 cm wide each) occurs. Pyrite and arsenopyrite are disseminated moderately.

(4) 101.85 – 106.50 m: White quartz-calcite vein/network zone, consisting of several white quartz veins/networks (1 to 49 cm wide each). Pyrite is disseminated in general. A small amount of sphalerite (light yellowish color) is spotted at about 106 m. A small amount of chalcopyrite, galena and pyrrhotite were observed under the microscope.

(5) 115.20 – 120.30 m: White quartz-calcite vein/network zone, consisting of more than 10 white quartz-calcite veins/networks (1 cm up to over 1 m wide each). Five significant quartz veins/networks were caught in this zone: 115.48 – 115.64, 116.67 – 117.95, 118.55 – 118.95, 119.08 – 119.60, and 119.95 – 120.30 m. Chlorite was observed partly. In these quartz veins/networks, a significant amount of pyrite and arsenopyrite are disseminated. These sulfide minerals are aggregated into small patches. A small amount of chalcopyrite and pyrrhotite were also found. Several grains of gold (some are coarse carat) were detected in slime of drilling.

(6) 126.25 – 132.10 m: White quartz-calcite vein/network zone, consisting of more than 10 white quartz-calcite veins/veinlets and networks (1 to 105 cm wide each). Two significant quartz veins/networks were caught in this zone: 126.25 – 127.30, and 131.65 – 132.10 m. In these quartz veins/networks, a significant amount of pyrite and arsenopyrite were observed. A small amount of chalcopyrite, sphalerite and pyrrhotite were observed under the microscope.

(7) 143.12 – 153.98 m: White quartz-calcite vein/network zone, consisting of more than 20 white quartz-calcite veins/networks or breccias (1 cm up to around 1 m wide each). Six significant quartz veins/networks were caught in this zone: 143.40 – 143.75, 145.53 – 145.88, 146.00 – 146.65, 147.00 – 147.55, 148.10 – 149.08, and 153.04 – 153.53 m. Chlorite was observed partly. In these quartz veins/networks, a significant amount of pyrite and arsenopyrite are disseminated (as patches). A small amount of chalcopyrite, galena and pyrrhotite were observed under the microscope. Several grains of gold (fine carat) were detected in slime of drilling.

(8) 254.00 – 256.40 m: Light gray quartz vein/network zone, consisting of light gray quartz-calcite veins/veinlets or networks (a few cm to 11 cm wide). Host rocks are generally silicified, occasionally clayey. Pyrite is weakly disseminated. Galena was observed in quartz.

2-7-5 Fluid Inclusion Studies

(1) Methodology

Quartz chips were collected, and provided for fluid inclusion studies. Ten quartz chips were sampled from drill cores in the third phase drilling. The breakdown is: 7 from MJVB-3 and 4 in the Da Mai area, and 3 from MJVB-5 and 6 in the Ngan Me area. All samples were taken from quartz veins. The same methods and measurements as in the detailed geological survey were made for the studies.

(2) Results of Studies

The total number of fluid inclusions which were investigated under the microscope was 243*. More than eighty percents of them are liquid-rich two-phase inclusions. Gas-rich two-phase inclusions are less than 20 % of them. This result may indicate that the boiling of fluid has occurred locally during the formation of quartz vein.

Polyphase inclusions were found in 4 samples. The solid phase looked like halite, but it was difficult to identify because the fluid inclusions were very small.

Homogenization Temperature

Values of homogenization temperature of each fluid inclusion are distributed from 142°C to 386°C. Most of them fall into a range of 180° ~ 300°C with a peak value of around 200°C.

Salinity

Samples for the measurement of freezing temperature were selected from quartz chips of which homogenization temperature was measured. Eight measurements on salinity for 4 fluid inclusions from the drill cores MJVB-3, 4 and 5 were made in this study.

Salinity calculated from the freezing temperatures of fluid inclusions ranges from 1.6 to 6.3 wt. % NaCl equivalent. The arithmetic mean of three salinity values is 4.0 wt. % NaCl equiv.